Small-angle Bhabha scattering

A. B. Arbuzov and É. A. Kuraev
Joint Institute for Nuclear Research, Dubna

Fiz. Élem. Chastits At. Yadra **27**, 1247–1320 (September–October 1996)

The present status of the theoretical description of electron–positron scattering at small angles is reviewed. A detailed description is given of an approach which allows the theoretical uncertainty to be reduced to 0.1%, corresponding to the accuracy required for precise determination of the luminosity at LEP I. This accuracy is obtained by exact inclusion of the radiative corrections in first-order perturbation theory and the logarithmic contributions in the second order. The third-order contributions are taken into account in the leading-log approximation. The results of numerical calculations for the experimental conditions of LEP I are presented and compared with the results of other groups. [S1063-7796(96)00205-7]

1. INTRODUCTION

The cross section σ for any process occurring in an electron–positron collider is defined as the ratio of the number of events per second N and the luminosity $\mathscr{L}$: $\sigma = N/\mathscr{L}$. The luminosity is one of the fundamental characteristics of a collider. It is determined by measuring the number of events per second N_1 of a process whose cross section σ_1 is well known theoretically: $\mathscr{L} = N_1/\sigma_1$. To decrease the statistical error, the cross section for this reference process should satisfy the following requirements: it should be fairly large, and the corresponding events should admit reliable identification. For accelerators operating at intermediate energies with a small number of electrons (positrons) per bunch ($\lesssim 10^{13}$), the reference process is usually chosen to be double bremsstrahlung in different directions. However, as the number of particles per bunch increases, this process becomes unfavorable, owing to the large probability of it being mimicked by two unrelated single bremsstrahlung processes occuring when bunches collide. Another process used to determine the luminosity at electron–positron colliders is e^+e^- scattering (Bhabha scattering). Large-angle Bhabha scattering events are selected in the case of colliders operating at moderately high energy (Φ and Ψ factories) with total beam energy $\sqrt{s} = 2\varepsilon \lesssim 1-3$ GeV. Muon pair production and annihilation into photons are also sometimes used. In the case of high-energy colliders like LEP I and LEP II in Geneva, small-angle (less than 100 mrad) Bhabha scattering (SABS) is more useful. The cross section for this process does not fall off with increasing beam energy ε, owing to the dominant contribution from t-channel graphs (we shall work in the center-of-mass frame of the initial particles). The cross sections of both the elastic and some of the inelastic processes contributing to the experimentally measured number of events can now in principle be calculated to any precision, using the well developed theory of the electroweak interaction. Moreover, except for small hadronic corrections and small effects from the interference of the amplitudes of photon and Z-boson exchange, the calculations can be performed using quantum electrodynamics. For a generally applicable determination of the experimental luminosity it is important that at sufficiently small electron and positron scattering angles at an energy near $\sqrt{s} = M_Z$, the rate of counting SABS events at LEP I is much higher than the rate of counting the number of Z-boson production events.

The experimental precision of measuring the luminosity is steadily improving. During the initial period of operation of LEP I it was about 1%. Now it is already 0.07% (significantly better than the accuracy that was planned), and it is quite possible that in the near future it will be improved further to 0.05%. Is it possible to reduce the uncertainty of the *theoretical* calculation of the cross section for the SABS process to the experimental level, taking into account the actual experimental conditions? Apparently, it is. Special attention has been given to this problem recently (see Ref. 1 and references therein). It should be noted that a highly accurate theoretical calculation of the cross section for Bhabha scattering is also needed for precision tests of the Standard Model, because this process gives the absolute normalization of all the processes occurring at LEP. The present review is devoted to the theoretical calculation of the cross section for SABS processes, taking into account the experimental conditions with guaranteed precision

$$\frac{\Delta\sigma_{\text{theor}}}{\sigma} \lesssim 0.1\%. \qquad (1)$$

The approaches to the theoretical description of the SABS cross section can be divided into two classes. The first involves the accurate inclusion of radiative corrections in lowest-order perturbation theory and the use of approximation formulas for including higher-order perturbative contributions. Monte Carlo methods play an important role in the calculations of the cross sections for inelastic processes, as they are used to obtain numerical results for specific experimental conditions. There is a large literature on this approach. The most successful work in this area is that of the group of Jadach,[2,3] based on the use of the exponentiation procedure for including the main corrections from higher-order perturbation theory for the differential cross sections. The results of this group were used to analyze the LEP I data during the period when the experimental precision was worse than 0.25%, i.e., before 1991. By now the experimental precision has been increased by at least a factor of four, so that the requirements on the precision of the theoretical

 1063-7796/96/050510-29$10.00

calculation have accordingly become more stringent. The use of approximation formulas like exponentiation formulas, which are consistent with the more general structure-function approach only in a special case, no longer ensures the required precision.

The second approach,[4] which is what we mainly focus on here, is the analytic calculation of the nonleading contributions through the second order of perturbation theory. The advantage of this approach is the possibility of calculating the nonleading contributions exactly. The drawback is the need for an independent calculation of the contributions of inelastic processes when the experimental setup (the conditions under which the final particles are detected) is changed. The first approach has the definite advantage that the Monte Carlo method can be used for any experimental conditions, and its drawback is the fact that the nonleading contributions are not taken into account exactly.

The exact results from first-order perturbation theory have been successfully combined with the structure-function technique in the studies by the Nicrosini and Caffo groups.[5,6] Integration using the Monte Carlo method with weighted events was used to take into account the experimental conditions as accurately as possible. A special technique was used to smooth out the peaks in the integrand. The higher-order nonleading contributions were also estimated.

The cross section for the SABS process is calculated in the Standard Model, with the dominant contributions obtained using perturbative QED. It turns out that it is sufficient to include the contributions from the heavy Z and W vector bosons using only the Born approximation. In addition to the elastic scattering process (including *soft* photons and e^+e^- pairs not detected experimentally), it is necessary to include also various inelastic processes: the emission of an additional hard photon, two hard photons, the production of hard electron–positron pairs, and so on. The differential cross sections for these processes must be integrated over the phase space of the emitted additional particles with constraints corresponding to the actual experimental conditions.

Like any high-energy process involving light charged fermions, the SABS process has relatively large (of order several percent) radiative corrections of QED origin.

We stress the fact that since the procedure for subtracting QED effects is applied to experimental quantities, all the uncertainties of the QED calculation directly become the systematic errors. In the case of recent experiments at LEP, the QED component of the systematic experimental errors in determining the luminosity was the same as the systematic error from the apparatus.

If the QED uncertainty is this important, the question arises of where it comes from and how to decrease it. Following the authors of Ref. 3, we distinguish two equally important sources. The first is the *technical precision*—the errors due to numerical approximations and inaccuracies in the analytic and numerical calculations. The second is higher-order effects, new physics, and so on, i.e., the nonleading contributions. This is the *physical precision*. The full QED uncertainty is the sum (in quadratures) of the technical and physical precisions.

The technical precision is estimated in various ways, for example, by using two different Monte Carlo programs. The results are compared, and attempts are made to reduce the errors. The Jadach group has achieved a technical accuracy of 0.02% in this way.

A source of physical precision is the calculation of higher-order perturbative effects and the estimation of the discarded terms. It should be noted that reliably estimating the technical and physical precision is just as difficult as actually calculating them.

The only way of obtaining the physical precision in the calculation of higher-order effects is by explicitly determining the terms which are usually neglected. It is this approach that the present authors have worked on. In the approach of the Jadach group, an upper limit on the *small* contributions is obtained. In that approach it is often necessary to develop original computational techniques and to write new Monte Carlo programs. Nevertheless, they have succeeded in formulating and solving the problem of decreasing the uncertainties to 0.25%. This was achieved by combining semianalytical calculations and new Monte Carlo programs, and the result of first-order perturbation theory was reproduced exactly. The second-order calculation was actually reduced to the inclusion of leading terms of the form $(\alpha/\pi)^2L^2$, where L is the so-called *large* logarithm, $L=\ln(t_0/m_e^2)$, and t_0 is the square of the typical momentum transfer ($L\approx 15$ for the conditions of LEP), and to the estimation of the nonleading contributions of the form $(\alpha/\pi)^2L$ and the contribution of pair production. For example, for the nonleading contributions from photon emission the uncertainty was 0.2%, and for that from pair production it was 0.1%. Taking into account also the uncertainty due to vacuum polarization by hadrons (0.08%) and the technical uncertainty, a total theoretical uncertainty of 0.25% was obtained.

Let us say a few words about the Yennie–Frautschi–Suura (YFS) exponentiation procedure,[7] which has been used intensively by the Jadach group. It is described in detail in Ref. 3 (see references therein). The authors constructed a certain synthetic expression [see Eq. (2) in Ref. 3] for describing (virtual and real) photon emission. It is the product, integrated over final fermion states (taking into account the experimental constraints), of the known YFS factor describing the emission of virtual and soft (with energy less than several times Ω) photons and the infinite sum over the number of emitted real photons (with energy greater than Ω) of a combination of accompanying-radiation factors with weights correctly reproducing the radiative corrections of first-order perturbation theory. The authors used Monte Carlo methods to study the dependence of this expression on the choice of the parameter Ω and on the agreement between the one-loop calculations and calculations of the cross sections for inelastic processes carried out by the CALKUL group.[8] This expression then became the fundamental component in the calculation of the physical QED uncertinties.

We have no doubt that this approach correctly describes the first-order corrections and is a good model for including higher orders of perturbation theory, at least in the leading approximation. However, we would like to make the following observations. The authors did not make any comparisons with the exact results for the double-bremsstrahlung and small-angle pair-production channels obtained in a series of studies from the 1970s (Ref. 9), where, in particular, it was pointed out that approximation by the accompanying-radiation factors is too crude in the case of hard-photon emission, and exact expressions were given. Secondly, we question the use of the Kinoshita–Lee–Nauenberg theorem. It guarantees the cancellation of the leading contributions of the virtual radiative corrections and the contributions arising from the inclusion of hard photons when the entire spectrum is integrated over, whereas in an experiment the energy of the final particles is bounded. Thirdly, the production of light fermion pairs is not described by such expressions and, in the best case, was described by the authors using the structure-function approximation. Our approach to the inclusion of the *physical uncertainties*, which is presented in detail below, amounts to calculating them explicitly. We calculate the nonleading contributions of order $(\alpha/\pi)^2 L$ from both photon-emission and pair-production processes.

The use of small angles leads to some advantages in performing the calculations. For example, terms of order $\theta^2 = 4|t|/s$ in the calculation of higher orders of perturbation theory can, as a rule, be dropped, although they must be included in the Born approximation. In particular, in the case of small-angle scattering it becomes possible to neglect the entire class of corrections originating in so-called *up–down interference.*

Here we mean the contribution to the correction to the cross section proportional to $\theta^2(\alpha/\pi)^n$ ($n=1$, 2) and originating in the interference of the amplitudes describing the emission of real photons and pairs along the directions of the initial electron and positron beams. A similar phenomenon occurs when including the exchange of several photons in the t channel in the case of elastic scattering, where the *generalized eikonal representation* holds for the amplitude. The exact amplitude of the process involving multiphoton exchange differs from the amplitude in the Born approximation by the phase factor $\exp\{i\phi\}$ and the presence of the form factors:[10]

$$A(t) = A_0(t)(\Gamma(t))^2 e^{i\phi(t)}\left(1 + \mathscr{O}\left(\frac{\alpha t}{\pi s}\right)\right).$$

Calculating the contributions to the radiative correction of order (α/π) with power-law accuracy [i.e., neglecting terms of order $\mathscr{O}(m^2/|t|)$] and also the contributions of order $(\alpha/\pi)^2$ in the logarithmic approximation (i.e., keeping only terms containing the large logarithm L), we have confirmed the validity of the parton representation (i.e., the representation in the form of a cross section for a process of the Drell–Yan type) for the cross section of the SABS process in the leading-log approximation [i.e., keeping only corrections $\sim(\alpha L/\pi)^n$]. In addition, the nonleading contributions of order (α/π) and $(\alpha/\pi)^2 L$ have been obtained explicitly. Their form cannot be determined using the renormalization-group formalism, which determines the form of the cross section in the leading-log approximation.

The corrections due to the emission of virtual and real electron–positron pairs also must be taken into account with the required accuracy. Here again we have found that the leading contributions $\sim(\alpha L/\pi)^2$ agree with the parton representation, and that the nonleading contributions must be taken into account in estimating the accuracy. In general, the leading contributions to the cross section can be obtained in the renormalization-group approximation by iteration of the Lipatov equations[11–14] (see Appendix G).

Knowledge of these contributions allows the accuracy of the calculations of the radiative corrections to the differential cross section in the Born approximation $d\sigma_0$ to be guaranteed as

$$d\sigma = d\sigma_0(1+\delta), \quad \delta = \delta_{\text{lead}} + \delta_{\text{nonlead}} + \Delta\delta,$$
$$\Delta\delta < 0.1\%, \tag{2}$$

where δ_{lead} is the contribution of the leading-log approximation, and δ_{nonlead} is the contribution of the next-to-leading-log approximation. The quantity $\Delta\delta$ contains neglected contributions of the type

$$\left(\frac{\alpha}{\pi}\right)^2, \quad \left(\frac{\alpha}{\pi}\right)^3 L^2, \quad \frac{\alpha}{\pi}\theta^2, \quad \frac{m^2L^2}{|t|}, \quad \ldots .$$

We have also neglected the contributions of higher orders due to the production of pairs of heavy particles (pions, muons, and so on; see Sec. 8).

We recall that accurate measurement of the luminosity and cross sections is just as important for the precision verification of the Standard Model. It is well known that the measurement of the invisible Z-boson decay channels parametrized in terms of the number of neutrino types N_ν depends directly on the error in measuring the luminosity, $\delta\mathscr{L}/\mathscr{L}$. Since N_ν and $\sigma_{\text{tot}}(M_Z)$ depend very weakly on the details of the Standard Model, in particular, on the masses of the Higgs boson and the top quark, a marked difference of N_ν from 3 would signal *new physics* beyond the Standard Model. The value of $\delta\mathscr{L}/\mathscr{L}$ also directly affects the accuracy of measuring the electron–positron width of the Z boson and, accordingly, the accuracy of measuring the electroweak mixing angle.

In Sec. 2 we discuss the experimental setup with symmetrically arranged small-aperature ring detectors. There we also present the known results for the cross section in the Born approximation calculated using the Standard Model. In Sec. 3 we study the radiative correction due to the emission of a single real or virtual photon. In Secs. 4 and 5 we calculate the radiative corrections of order α^2 due to the emission of two photons (real or virtual) and to (real or virtual) electron–positron pair production, respectively. The contribution of leading terms of the form $(\alpha L/\pi)^3$ is given in Sec. 6. In Sec. 7 we study the *calorimetric experimental setup.* In Sec. 8 we analyze the discarded terms and the accuracy of the calculations. In the conclusion we analyze the results numerically and discuss them. In the appendices we derive the cross section for single bremsstrahlung using the Sudakov technique; we give the details of the calculations of the virtual corrections to single bremsstrahlung; we calculate the contribution of semicollinear kinematics to double bremsstrahlung; we demonstrate the cancellation of the Δ dependence in the nonleading contributions; we give the representation of the leading contributions in terms of structure functions; we analyze the case of nonsymmetric detectors; and we iterate the Lipatov equations.

2. FORMULATION OF THE PROBLEM AND THE CROSS SECTION IN THE BORN APPROXIMATION

We shall study the reaction

$$e^-(p_1)+e^+(p_2)\to e^-(q_1)+e^+(q_2)+(n\gamma)+(e^+e^-) \tag{3}$$

in the inclusive case, i.e., the simultaneous detection of an electron and a positron by two detectors in opposite directions is considered to be a Bhabha event. We consider the energy range typical of the LEP I and LEP II setups: $2\varepsilon=\sqrt{s}=90-200$ GeV, where ε is the energy of the incident particle in the c.m. frame. Generalization of the results to other energy ranges will require additional analysis of the contribution of the discarded terms. The following experimental constraints are imposed on the scattering angles:

$$\theta_1<\theta_-=\widehat{\mathbf{p}_1\mathbf{q}_1}\equiv\theta<\theta_3,\quad \theta_2<\theta_+=\widehat{\mathbf{p}_2\mathbf{q}_2}<\theta_4,$$
$$0.01\lesssim\theta_i\lesssim 0.1\ \text{rad}, \tag{4}$$

where $\mathbf{p}_1$ and $\mathbf{q}_1$ ($\mathbf{p}_2$ and $\mathbf{q}_2$) are the momenta of the initial and scattered electron (positron). In the case of symmetric ring detectors we have $\theta_1=\theta_2$ and $\theta_3=\theta_4$. In analyzing the observed events we impose an additional condition on the energy of the detected particles:

$$x_1x_2<x_c,\quad x_{1,2}=\frac{q^0_{1,2}}{\varepsilon}, \tag{5}$$

where x_1 and x_2 are the energy fractions of the final electron and positron, and x_c is a parameter selected from analysis of the experimental data $(0<x_c<1)$. By the experimentally observed cross section $\sigma_{\rm exp}$ we mean the cross section for the process (3) integrated in a given angular range, taking into account the condition (5). Other experimental setups are also possible in practice. For example, in the calorimetric setup, which will be discussed in Sec. 7, when two or more particles are simultaneously incident on a small area of the detector they will be detected as a single particle with energy equal to the sum of the energies of all the particles forming the *cluster*. In our calculations we shall assume that the detector distinguishes between charged and neutral particles; otherwise, it would be necessary to allow for the possibility of events in which one or both charged final particles mimic photons. In any case, the scheme that we propose for calculating the radiative corrections can be modified to fit a very wide range of experimental situations.

For the small scattering angles that we consider we can expand the expression for the cross section in a series in powers of the scattering angle. The leading contribution to the differential cross section $d\sigma/d\theta^2$ comes from graphs with one-photon exchange in the t channel. This contribution has a θ^{-4} singularity for $\theta\to 0$. Let us estimate the correction of relative order θ^2 to this contribution. If

$$\frac{d\sigma}{d\theta^2}\sim\theta^{-4}(1+c_1\theta^2), \tag{6}$$

then after integration over θ^2 with the limits (4) we obtain

$$\int_{\theta_1^2}^{\theta_3^2}\frac{d\sigma}{d\theta^2}\,d\theta^2\sim\theta_1^{-2}\left(1+c_1\theta_1^2\ln\frac{\theta_3^2}{\theta_1^2}\right).$$

For $\theta_1=50$ mrad and $\theta_3=150$ mrad, the relative contribution of this correction will be of order $2.5\times10^{-3}c_1$. Therefore, terms of relative order θ^2 must be kept only in working in the Born approximation, where c_1 is not small. In higher orders of perturbation theory the coefficient c_1 contains the small factor α/π, which allows such contributions to be discarded. This means that in the angular range of interest at a given accuracy, radiative corrections arise only from Feynman graphs of the scatterer type. Moreover, in calculating the radiative corrections we should consider only the contributions from graphs with exchange of a single photon in the t channel owing to the generalized eikonal representation.[10]

Taking into account the fact that the minimum value of the modulus of the squared momentum transfer $|t|=Q^2=2\varepsilon^2(1-\cos\theta)$ is of order 1 GeV^2, we shall neglect, without loss of accuracy, terms proportional to m^2/Q^2 (where m is the electron mass), and also the analogous terms of the type m_μ^2/Q^2 arising in the calculation of the radiative corrections.

The cross section for Bhabha scattering in the Born approximation in the Standard Model is well known:[15]

$$\frac{d\sigma^B}{d\Omega}=\frac{\alpha^2}{8s}\{4B_1+(1-c)^2B_2+(1+c)^2B_3\}, \tag{7}$$

where

$$B_1=\left(\frac{s}{t}\right)^2|1+(g_v^2-g_a^2)\xi|^2,\quad B_2=|1+(g_v^2-g_a^2)\chi|^2,$$

$$B_3=\frac{1}{2}\left|1+\frac{s}{t}+(g_v+g_a)^2\left(\frac{s}{t}\,\xi+\chi\right)\right|^2+\frac{1}{2}\left|1+\frac{s}{t}+(g_v-g_a)^2\left(\frac{s}{t}\,\xi+\chi\right)\right|^2,$$

$$\chi=\frac{\Lambda s}{s-M_Z^2+iM_Z\Gamma_Z},\quad \xi=\frac{\Lambda t}{t-M_Z^2},$$

$$\Lambda=\frac{G_FM_Z^2}{2\sqrt{2}\pi\alpha}=(\sin 2\theta_w)^{-2},$$

$$g_a=-\frac{1}{2},\quad g_v=-\frac{1}{2}(1-4\sin^2\theta_w),$$

$$s=(p_1+p_2)^2=4\varepsilon^2,$$

$$t=-Q^2=(p_1-q_1)^2=-\frac{1}{2}s(1-c),$$

$$c=\cos\theta,\quad \theta=\widehat{\mathbf{p}_1\mathbf{q}_1}.$$

Here θ_w is the Weinberg angle. For small angles, expanding (7), we find

$$\frac{d\sigma^B}{\theta d\theta}=\frac{8\pi\alpha^2}{\varepsilon^2\theta^4}\left(1-\frac{\theta^2}{2}+\frac{9}{40}\theta^4+\delta_{\rm weak}\right),$$

where $\varepsilon=\sqrt{s}/2$ is the initial electron (positron) energy in the c.m. frame. The correction δ_{weak} is associated with the contribution of graphs with Z-boson exchange, and can be written as

$$\delta_{\text{weak}}=2g_v^2\xi-\frac{\theta^2}{4}(g_v^2+g_a^2)\text{Re}\chi+\frac{\theta^4}{32}(g_v^4+g_a^4+6g_v^2g_a^2)|\chi|^2. \tag{8}$$

We see from (8) that the corresponding contribution c_1^W to the coefficient c_1 introduced in (6) is given by

$$c_1^W\lesssim 2g_v^2+\frac{(g_v^2+g_a^2)}{4}\frac{M_Z}{\Gamma_Z}+\theta_{\max}^2\frac{(g_v^4+g_a^4+6g_v^2g_a^2)}{32}\frac{M_Z^2}{\Gamma_Z^2}\simeq 1. \tag{9}$$

According to the above arguments, this implies that at the Born level the contribution of Z-boson exchange is less than 0.3%. Therefore, graphs with radiative corrections including Z-boson exchange can be discarded, because their contribution is less than 0.01%.

3. $\mathcal{O}(\alpha)$ RADIATIVE CORRECTIONS TO BHABHA SCATTERING

First let us consider the corrections due to the emission of a single virtual or soft photon. In the case of pure electrodynamics the one-loop radiative corrections to the cross section for Bhabha scattering have been calculated many years ago.[16] Taking into account the contribution due to the emission of a soft photon with energy below some small finite value $\Delta\varepsilon$, this one-loop correction can be written as

$$\frac{d\sigma_{\text{QED}}^{(1)}}{dc}=\frac{d\sigma_{\text{QED}}^{B}}{dc}(1+\delta_{\text{virt}}+\delta_{\text{soft}}), \tag{10}$$

where $d\sigma_{\text{QED}}^B$ is the Born cross section in the case of pure QED (it is $d\sigma^B$ for $g_a=g_v=0$), and

$$\begin{aligned}\delta_{\text{virt}}+\delta_{\text{soft}}=2\frac{\alpha}{\pi}\Bigg[&2\left(1-\ln\left(\frac{4\varepsilon^2}{m^2}\right)+2\ln\left(\cot\frac{\theta}{2}\right)\right)\ln\frac{\varepsilon}{\Delta\varepsilon}+\int_{\cos^2\theta/2}^{\sin^2\theta/2}\frac{dx}{x}\ln(1-x)-\frac{23}{9}\\&+\frac{11}{6}\ln\left(\frac{4\varepsilon^2}{m^2}\right)\Bigg]+\frac{\alpha}{\pi}\frac{1}{(3+c^2)^2}\Bigg[\frac{\pi^2}{3}(2c^4-3c^3-15c)+2(2c^4-3c^3+9c^2+3c\\&+21)\ln^2\left(\sin\frac{\theta}{2}\right)-4(c^4+c^2-2c)\ln^2\left(\cos\frac{\theta}{2}\right)-4(c^3+4c^2+5c\\&+6)\ln^2\left(\tan\frac{\theta}{2}\right)+\frac{2}{3}(11c^3+33c^2+21c+111)\ln\left(\sin\frac{\theta}{2}\right)+2(c^3-3c^2+7c\\&-5)\ln\left(\cos\frac{\theta}{2}\right)+2(c^3+3c^2+3c+9)\delta_t-2(c^3+3c)(1-c)\delta_s\Bigg].\end{aligned}$$

The quantity δ_t (δ_s) is determined in terms of the contribution to the photon vacuum-polarization operator $\Pi(t)$ [$\Pi(s)$]:

$$\Pi(t)=\frac{\alpha}{\pi}\left(\delta_t+\frac{1}{3}\ln\frac{Q^2}{m^2}-\frac{5}{9}\right)+\frac{1}{4}\left(\frac{\alpha}{\pi}\right)^2\ln\frac{Q^2}{m^2},$$

where

$$Q^2=-t=2\varepsilon^2(1-c),\quad \delta_s=\delta_t(Q^2\to -s).$$

We have kept only the leading part of the two-loop contribution to the polarization operator. In the Standard Model δ_t contains the contributions of muons, τ leptons, W bosons, and hadrons:

$$\delta_t=\delta_t^\mu+\delta_t^\tau+\delta_t^W+\delta_t^H.$$

The first three contributions can be calculated theoretically:

$$\delta_t^\mu=\frac{1}{3}\ln\frac{Q^2}{m_\mu^2}-\frac{5}{9},$$

$$\delta_t^\tau=\frac{1}{2}v_\tau\left(1-\frac{1}{3}v_\tau^2\right)\ln\frac{v_\tau+1}{v_\tau-1}+\frac{1}{3}v_\tau^2-\frac{8}{9},$$

$$v_\tau=\sqrt{1+\frac{4m_\tau^2}{Q^2}},$$

$$\delta_t^W=\frac{1}{4}v_W(v_W^2-4)\ln\frac{v_W+1}{v_W-1}-\frac{1}{2}v_W^2+\frac{11}{6},$$

$$v_W=\sqrt{1+\frac{4m_W^2}{Q^2}}.$$

The hadron contribution to the vacuum polarization can be represented as an integral of the experimentally measured cross section for electron–positron annihilation into hadrons:

$$\delta_t^H=\frac{Q^2}{4\pi\alpha^2}\int_{4m_\pi^2}^{+\infty}\frac{\sigma^{e^+e^-\to h}(x)}{x+Q^2}\,dx.$$

In the numerical calculations we use the parametrization of $\Pi(t)$ suggested in Ref. 17.

In the limit of small scattering angles we can write (10) as

$$\frac{d\sigma_{\text{QED}}^{(1)}}{dc}=\frac{d\sigma_{\text{QED}}^{B}}{dc}(1-\Pi(t))^{-2}(1+\delta),$$

$$\delta=2\frac{\alpha}{\pi}\left[2(1-L)\ln\frac{1}{\Delta}+\frac{3}{2}L-2\right]+\frac{\alpha}{\pi}\theta^2\Delta_\theta+\frac{\alpha}{\pi}\theta^2\ln\Delta,$$

$$\Delta_\theta=\frac{3}{16}l^2+\frac{7}{12}l-\frac{19}{18}+\frac{1}{4}(\delta_t-\delta_s),$$

$$\Delta=\frac{\Delta\varepsilon}{\varepsilon},\quad l=\ln\frac{Q^2}{s}\simeq\ln\frac{\theta^2}{4}. \tag{11}$$

This representation allows us to verify explicitly the statement that the contribution of terms of relative order θ^2 to the radiative corrections is small. Taking into account the fact that the terms of large magnitude proportional to $\ln\Delta$ cancel when added to the contribution from hard-photon emission, it can be verified that the contribution to the coefficient c_1 from these one-loop corrections is small. In what follows we shall systematically discard the contributions to the radiative corrections from annihilation graphs and also from graphs with exchange of several photons in the t channel. The latter follows from the generalized eikonal representation, which is applicable for small scattering angles. In particular, in the case of elastic scattering we have[10]

$$A(s,t)=A_0(s,t)F_1^2(t)(1-\Pi(t))^{-1}\mathrm{e}^{i\varphi(t)}\left[1+\mathcal{O}\left(\frac{\alpha Q^2}{\pi s}\right)\right],\quad s\gg Q^2\gg m^2, \tag{12}$$

where $A_0(s,t)$ is the Born amplitude, $F_1(t)$ is the Dirac form factor of the electron, and $\varphi(t)=-\alpha\,\ln(Q^2/\lambda^2)$ is the known *Coulomb phase*. Here and below, λ is an auxiliary parameter introduced as the photon mass. The eikonal representation is violated at the three-loop level, but the corresponding contribution to the cross section for this process is quite small ($\sim\alpha^5$) and can be dropped. We can thus regard the generalized eikonal representation as valid within the accuracy to which we are working.[1)]

Now we introduce the dimensionless quantity $\Sigma=(Q_1^2\sigma_{\exp})/(4\pi\alpha^2)$, where $Q_1^2=\varepsilon^2\theta_1^2$ and $\sigma_{\exp}$ denotes the experimentally observed cross section:

$$\Sigma=\frac{Q_1^2}{4\pi\alpha^2}\int dx_1\int dx_2\Theta(x_1x_2-x_c)\int d^2\mathbf{q}_1^\perp\Theta_1^c\int d^2\mathbf{q}_2^\perp\Theta_2^c\times\frac{d\sigma\{e^++e^-\to e^+(\mathbf{q}_2^\perp,x_2)+e^-(\mathbf{q}_1^\perp,x_1)+X\}}{dx_1d^2\mathbf{q}_1^\perp dx_2d^2\mathbf{q}_2^\perp},$$

where $x_{1,2}$ and $\mathbf{q}_{1,2}^\perp$ denote the energy fractions and components of the momenta of the final electron (subscript 1) and positron (subscript 2) perpendicular to the axis of the initial beams. The quantity sx_c denotes the experimental cutoff in the square of the invariant mass of the detected particles. The generalized functions $\Theta_{1,2}^c$ specify the limits of integration over the angles (4):

$$\Theta_1^c=\Theta\left(\theta_3-\frac{|\mathbf{q}_1^\perp|}{x_1\varepsilon}\right)\Theta\left(\frac{|\mathbf{q}_1^\perp|}{x_1\varepsilon}-\theta_1\right),$$

$$\Theta_2^c=\Theta\left(\theta_4-\frac{|\mathbf{q}_2^\perp|}{x_2\varepsilon}\right)\Theta\left(\frac{|\mathbf{q}_2^\perp|}{x_2\varepsilon}-\theta_2\right).$$

In the case of an experimental setup symmetric in the positron and electron emission angles, we can introduce the parameter ρ:

$$\rho=\frac{\theta_3}{\theta_1}=\frac{\theta_4}{\theta_2}>1.$$

We write Σ as the sum of these contributions:

$$\Sigma=\Sigma_0+\Sigma^{\gamma}+\Sigma^{2\gamma}+\Sigma^{e^+e^-}+\Sigma^{3\gamma}+\Sigma^{e^+e^-\gamma}, \tag{13}$$

where Σ_0 denotes the modified Born cross section, Σ^γ is the contribution from the emission of a single (real or virtual) photon, and so on. We have modified the first term of the perturbation series by explicitly introducing the vacuum polarization of a virtual photon in the t channel:

$$\Sigma_0=\theta_1^2\int_{\theta_1^2}^{\theta_2^2}\frac{d\theta^2}{\theta^4}(1-\Pi(t))^{-2}+\Sigma_W+\Sigma_\theta, \tag{14}$$

where Σ_W is the correction from electroweak interactions:

$$\Sigma_W=\theta_1^2\int_{\theta_1^2}^{\theta_2^2}\frac{d\theta^2}{\theta^4}\delta_{\text{weak}}, \tag{15}$$

and the term Σ_θ reflects the inclusion of the following terms of the expansion in powers of θ^2 of the exact expression for the cross section in the Born approximation:

$$\Sigma_\theta=\theta_1^2\int_1^{\rho^2}\frac{dz}{z}(1-\Pi(-zQ_1^2))^{-2}\left(-\frac{1}{2}+z\theta_1^2\frac{9}{40}\right). \tag{16}$$

Below, we shall consider the other contributions to Σ.

Let us now study the contribution from the emission of a single hard photon. We write the differential cross section for the single-bremsstrahlung process in Bhabha scattering in terms of the energy fractions $x_{1,2}$ and the transverse components of the final particle momenta as[9] (see Appendix A)

$$\frac{d\sigma_B^{e^+e^-\to e^+e^-\gamma}}{dx_1d^2\mathbf{q}_1^\perp dx_2d^2\mathbf{q}_2^\perp}=\frac{2\alpha^3}{\pi^2}\left\{\frac{R(x_1;\mathbf{q}_1^\perp,\mathbf{q}_2^\perp)\delta(1-x_2)}{(\mathbf{q}_2^{\perp2})^2(1-\Pi(-\mathbf{q}_2^{\perp2}))^2}+\frac{R(x_2;\mathbf{q}_2^\perp,\mathbf{q}_1^\perp)\delta(1-x_1)}{(\mathbf{q}_1^{\perp2})^2(1-\Pi(-\mathbf{q}_1^{\perp2}))^2}\right\}(1+\mathcal{O}(\theta^2)), \tag{17}$$

where

$$R(x;\mathbf{q}_1^\perp,\mathbf{q}_2^\perp)=\frac{1+x^2}{1-x}\left[\frac{\mathbf{q}_2^{\perp2}(1-x)^2}{d_1d_2}-\frac{2m^2(1-x)^2x}{1+x^2}\frac{(d_1-d_2)^2}{d_1^2d_2^2}\right],$$

$$d_1=m^2(1-x)^2+(\mathbf{q}_1^\perp-\mathbf{q}_2^\perp)^2,$$

$$d_2=m^2(1-x)^2+(\mathbf{q}_1^\perp-x\mathbf{q}_2^\perp)^2. \tag{18}$$

Here we have again used the vacuum-polarization correction in the propagator of the virtual photon in the t channel. Performing the trivial integration over the azimuthal angle in (17), we obtain the contribution from the emission of a single hard photon Σ^H:

$$\Sigma^H=\frac{\alpha}{\pi}\int_{x_c}^{1-\Delta}dx\,\frac{1+x^2}{1-x}F(x,D_1,D_3;D_2,D_4), \tag{19}$$

where

$$F=\int_{D_1}^{D_3}dz_1\int_{D_2}^{D_4}\frac{dz_2}{z_2}(1-\Pi(-z_2Q_1^2))^{-2}\left\{\frac{1-x}{z_1-xz_2}\right.$$

$$\left.\times(a_1^{-1/2}-xa_2^{-1/2})-\frac{4x\sigma^2}{1+x^2}[a_1^{-3/2}+x^2a_2^{-3/2}]\right\},$$

$$a_1=(z_1-z_2)^2+4z_2\sigma^2,\quad a_2=(z_1-x^2z_2)^2$$

$$+4x^2z_2\sigma^2,\quad \sigma^2=\frac{m^2}{Q_1^2}(1-x)^2.$$

The limits of integration in the case of symmetric detectors are

$$D_1=x^2,\quad D_2=1,\quad D_3=x^2\rho^2,\quad D_4=\rho^2. \tag{20}$$

We rewrite this contribution in the final form (the details are given in Appendix A)

$$\Sigma^H=\frac{\alpha}{\pi}\int_{x_c}^{1-\Delta}dx\frac{1+x^2}{1-x}\int_1^{\rho^2}\frac{dz}{z^2}(1-\Pi(-zQ_1^2))^{-2}\{[1$$

$$+\Theta(x^2\rho^2-z)](L-1)+k(x,z)\},$$

$$k(x,z)=\frac{(1-x)^2}{1+x^2}[1+\Theta(x^2\rho^2-z)]+L_1+\Theta(x^2\rho^2$$

$$-z)L_2+\Theta(z-x^2\rho^2)L_3, \tag{21}$$

where $L=\ln(zQ_1^2/m^2)$ and

$$L_1=\ln\left|\frac{x^2(z-1)(\rho^2-z)}{(x-z)(x\rho^2-z)}\right|,\quad L_2=\ln\left|\frac{(z-x^2)(x^2\rho^2-z)}{x^2(x-z)(x\rho^2-z)}\right|,$$

$$L_3=\ln\left|\frac{(z-x^2)(x\rho^2-z)}{(x-z)(x^2\rho^2-z)}\right|. \tag{22}$$

From (21) we see that Σ^H contains the auxiliary parameter Δ. This parameter cancels, as it should, in the sum $\Sigma^\gamma=\Sigma^H+\Sigma^{V+S}$, where Σ^{V+S} is the contribution of soft and virtual photons obtained from (11). For the sum we have

$$\Sigma^\gamma=\frac{\alpha}{\pi}\int_1^{\rho^2}\frac{dz}{z^2}\int_{x_c}^1dx(1-\Pi(-zQ_1^2))^{-2}\left\{(L-1)P(x)\right.$$

$$\left.\times[1+\Theta(x^2\rho^2-z)]+\frac{1+x^2}{1-x}k(x,z)-\delta(1-x)\right\}, \tag{23}$$

where

$$P(x)=\left(\frac{1+x^2}{1-x}\right)_+=\lim_{\Delta\to0}\left\{\frac{1+x^2}{1-x}\Theta(1-x-\Delta)+\left(\frac{3}{2}\right.\right.$$

$$\left.\left.+2\ln\Delta\right)\delta(1-x)\right\} \tag{24}$$

is the known nonsinglet kernel of the evolution equations.

4. TWO-PHOTON EMISSION IN BHABHA SCATTERING

Let us consider the corrections from the emission of both real and virtual photons. First we analyze the virtual two-loop corrections $d\sigma_{VV}^{(2)}$ to the differential cross section for elastic scattering. Using the representation (12) and the loop expansion of the Dirac form factor of the electron F_1,

$$F_1=1+\frac{\alpha}{\pi}F_1^{(1)}+\left(\frac{\alpha}{\pi}\right)^2F_1^{(2)}, \tag{25}$$

we obtain

$$\frac{d\sigma_{VV}^{(2)}}{dc}=\frac{d\sigma_0}{dc}\left(\frac{\alpha}{\pi}\right)^2(1-\Pi(t))^{-2}[6(F_1^{(1)})^2+4F_1^{(2)}]. \tag{26}$$

The one-loop contribution to the form factor is well known:

$$F_1^{(1)}=(L-1)\ln\frac{\lambda}{m}+\frac{3}{4}L-\frac{1}{4}L^2-1+\frac{1}{2}\zeta_2,$$

$$\zeta_2=\sum_1^\infty n^{-2}=\frac{\pi^2}{6}. \tag{27}$$

The two-loop contribution can be found in Ref. 19. We shall find it convenient to represent it as

$$F_1^{(2)}=F_1^{\gamma\gamma}+F_1^{e^+e^-}, \tag{28}$$

where the term $F_1^{e^+e^-}$ is related to the vacuum polarization by e^+e^- pairs,

$$F_1^{e^+e^-}=-\frac{1}{36}L^3+\frac{19}{72}L^2-\left(\frac{265}{216}+\frac{1}{6}\zeta_2\right)L+\mathcal{O}(1), \tag{29}$$

$$F_1^{\gamma\gamma}=\frac{1}{32}L^4-\frac{3}{16}L^3+\left(\frac{17}{32}-\frac{1}{8}\zeta_2\right)L^2+\left(-\frac{21}{32}-\frac{3}{8}\zeta_2\right.$$

$$\left.+\frac{3}{2}\zeta_3\right)L+\frac{1}{2}(L-1)^2\ln^2\frac{m}{\lambda}+(L-1)\left[-\frac{1}{4}L^2\right.$$

$$\left.+\frac{3}{4}L-1+\frac{1}{2}\zeta_2\right]\ln\frac{\lambda}{m}+\mathcal{O}(1),$$

$$\zeta_3=\sum_1^\infty n^{-3}\approx1.2020569. \tag{30}$$

The auxiliary parameter λ (the photon mass) entering into these expressions cancels in the sum with the contribution from soft-photon emission:

$$\frac{d\sigma^{(2)}}{dc}=\frac{d\sigma_{VV}^{(2)}}{dc}+\frac{d\sigma_{SS}^{(2)}}{dc}+\frac{d\sigma_{SV}^{(2)}}{dc}. \tag{31}$$

The differential cross section $d\sigma_{SS}^{(2)}/dc$ corresponds to the emission of two soft photons, where the energy carried by each is less than $\Delta\varepsilon$ ($\Delta\ll1$):

$$d\sigma_{SS}^{(2)}=d\sigma_0\left(\frac{\alpha}{\pi}\right)^2(1-\Pi(t))^{-2}8\left[(L-1)\ln\frac{m\Delta}{\lambda}+\frac{1}{4}L^2\right.$$

$$\left.-\frac{1}{2}\zeta_2\right]^2. \tag{32}$$

The contribution from the emission of a single soft photon with the one-loop virtual correction is

$$d\sigma_{SV}^{(2)}=d\sigma_0\left(\frac{\alpha}{\pi}\right)^2(1-\Pi(t))^{-2}16F_1^{(1)}\left[(L-1)\ln\frac{m\Delta}{\lambda}+\frac{1}{4}L^2-\frac{1}{2}\zeta_2\right]. \qquad (33)$$

The contribution of this sum, except for the terms entering into $F_1^{e^+e^-}$, contains the large logarithm L to no higher than the second power. It has the form

$$\Sigma_{S+V}^{\gamma\gamma}=\Sigma_{VV}+\Sigma_{VS}+\Sigma_{SS}=\left(\frac{\alpha}{\pi}\right)^2\int_1^{\rho^2}\frac{dz}{z^2}(1-\Pi(-zQ_1^2))^{-2}R_{S+V}^{\gamma\gamma}. \qquad (34)$$

For convenience, we write $R_{S+V}^{\gamma\gamma}$ as a sum:

$$R_{S+V}^{\gamma\gamma}=r_{S+V}^{\gamma\gamma}+r_{S+V\gamma\gamma}+r_{S+V\gamma\gamma}^{\gamma},$$

$$r_{S+V}^{\gamma\gamma}=r_{S+V\gamma\gamma}=L^2\left(2\ln^2\Delta+3\ln\Delta+\frac{9}{8}\right)+L\left(-4\ln^2\Delta-7\ln\Delta+3\zeta_3-\frac{3}{2}\zeta_2-\frac{45}{16}\right),$$

$$r_{S+V\gamma}^{\gamma}=4\left[(L-1)\ln\Delta+\frac{3}{4}L-1\right]^2. \qquad (35)$$

The contribution of the form factor $F_1^{e^+e^-}$ will be studied below.

Let us now consider the corrections to the emission of a single hard photon due to the emission of a soft or virtual photon. Here we can distinguish two cases: in the first the two photons are emitted from the same fermion line, and in the second they are emitted from different lines. Superscripts will denote emission from an electron line, and subscripts will denote emission from a positron line:

$$d\sigma|_{H,(S+V)}=d\sigma^{H(S+V)}+d\sigma_{H(S+V)}+d\sigma_{(S+V)}^{H}+d\sigma_H^{(S+V)}. \qquad (36)$$

In the case of emission by different fermions we obtain

$$\Sigma_{(S+V)}^{H}+\Sigma_H^{(S+V)}=2\Sigma^H\left(\frac{\alpha}{\pi}\right)\left[(L-1)\ln\Delta+\frac{3}{4}L-1\right], \qquad (37)$$

where Σ^H is given by (21). A more complicated result is obtained when calculating the radiative corrections to the emission of a hard photon from the same fermion line. In this case the cross section can be obtained using the Compton tensor with a *heavy photon*,[20] describing the process

$$\gamma^*(q)+e^-(p_1)\to e^-(q_1)+\gamma(k)+(\gamma_{\text{soft}}). \qquad (38)$$

In the limit of small emission angles of the hard photon we have

$$d\sigma^{H(S+V)}=\frac{\alpha^4 dx d^2\mathbf{q}_1^\perp d^2\mathbf{q}_2^\perp}{4x(1-x)(\mathbf{q}_2^\perp)^4\pi^3}[(B_{11}(s_1,t_1)+x^2B_{11}(t_1,s_1))\eta+T],$$

$$T=T_{11}(s_1,t_1)+x^2T_{11}(t_1,s_1)+x(T_{12}(s_1,t_1)+T_{12}(t_1,s_1)),$$

$$\eta=2\left(L-\ln\frac{(\mathbf{q}_2^\perp)^2}{-u_1}-1\right)(2\ln\Delta-\ln x)+3L-\ln^2 x-\frac{9}{2}, \qquad (39)$$

where $\Delta=\Delta\varepsilon/\varepsilon\ll 1$ ($\Delta\varepsilon$ is the maximum energy of the soft photon);

$$B_{11}(s_1,t_1)=(-4(\mathbf{q}_2^\perp)^2)/(s_1t_1)-8m^2/s_1^2 \qquad (40)$$

is the needed Born component of the Compton tensor; and the invariants are defined as

$$s_1=2q_1k,\quad t_1=-2p_1k,\quad u_1=(p_1-q_1)^2,$$
$$s_1+t_1+u_1=q^2. \qquad (41)$$

The final result (see Appendix B) has the form

$$\Sigma^{H(S+V)}=\Sigma_{H(S+V)}=\frac{1}{2}\left(\frac{\alpha}{\pi}\right)^2\int_1^{\rho^2}\frac{dz}{z^2}\int_{x_c}^{1-\Delta}\frac{dx(1+x^2)}{1-x}L\left\{\left(2\ln\Delta-\ln x+\frac{3}{2}\right)[(L-1)(1+\Theta)+k(x,z)]+\frac{1}{2}\ln^2 x+(1+\Theta)[-2+\ln x-2\ln\Delta]+(1-\Theta)\left[\frac{1}{2}L\ln x+2\ln\Delta\ln x-\ln x\ln(1-x)-\ln^2 x-\mathrm{Li}_2(1-x)-\frac{x(1-x)+4x\ln x}{2(1+x^2)}\right]-\frac{(1-x)^2}{2(1+x^2)}\right\}, \qquad (42)$$

where $k(x,z)$ is given in (21) and $\Theta=\Theta(x^2\rho^2-z)$.

Let us now consider the double bremsstrahlung of hard photons in small-angle Bhabha scattering. Again we distinguish the cases where two photons are emitted from different fermion lines and where they are emitted from one fermion. The differential cross section in the first case can be obtained using the factorization of the cross section in the impact-parameter representation. It takes the form[9]

$$\frac{d\sigma^{e^+e^-\to(e^+\gamma)(e^-\gamma)}}{dx_1d^2\mathbf{q}_1^\perp dx_2d^2\mathbf{q}_2^\perp}=\frac{\alpha^4}{\pi^3}\int\frac{d^2\mathbf{k}^\perp}{\pi(\mathbf{k}^\perp)^4}(1-\Pi(-(\mathbf{k}^\perp)^2))^{-2}\times R(x_1;\mathbf{q}_1^\perp,\mathbf{k}^\perp)R(x_2;\mathbf{q}_2^\perp,-\mathbf{k}^\perp), \qquad (43)$$

where $R(x;\mathbf{q}^\perp,\mathbf{k}^\perp)$ is given in (18). The calculation of the corresponding contribution Σ_H^H to Σ is analogous to the calculations for the case of single bremsstrahlung of a hard photon. The result is

$$\Sigma_H^H=\frac{1}{4}\left(\frac{\alpha}{\pi}\right)^2\int_0^\infty dz\, z^{-2}(1-\Pi(-zQ_1^2))^{-2}$$
$$\times\int_{x_c}^{1-\Delta}dx_1\int_{x_c/x_1}^{1-\Delta}dx_2\,\frac{1+x_1^2}{1-x_1}\frac{1+x_2^2}{1-x_2}$$
$$\times\Phi(x_1,z)\Phi(x_2,z), \qquad (44)$$

where [see (22)]

$$\Phi(x,z)=(L-1)[\Theta(z-1)\Theta(\rho^2-z)+\Theta(z-x^2)\Theta(\rho^2x^2-z)]+L_3[-\Theta(x^2-z)+\Theta(z-x^2\rho^2)]+\left(L_2+\frac{(1-x)^2}{1+x^2}\right)\Theta(z-x^2)\Theta(x^2\rho^2-z)+\left(L_1+\frac{(1-x)^2}{1+x^2}\right)\Theta(z-1)\Theta(\rho^2-z)+(\Theta(1-z)-\Theta(z-\rho^2))\ln\left|\frac{(z-x)(\rho^2-z)}{(x\rho^2-z)(z-1)}\right|.$$

We shall use the technique developed by Merenkov when studying double bremsstrahlung in a single direction (from the same lepton line).[21,22] We shall distinguish the *collinear* and *semicollinear* kinematics of photon emission. In the first case all the emitted photons move inside a narrow cone about the direction of motion of one (the initial or final) of the charged particles. The angles between the photon momenta and one of the lepton momenta are smaller than some auxiliary parameter θ_0:

$$\theta_i\leqslant\theta_0\ll 1. \qquad (45)$$

In the semicollinear kinematic region of phase space only one of the created photons moves inside this cone (with the same angle θ_0), and the second moves outside all such cones (there are four cones altogether: two about the momenta of the initial particles and two about the momenta of the final particles). This distinction has no physical meaning for a fully inclusive definition of the scattering cross section, and the parameter θ_0 cancels in the final result. However, it is possible to have experimental conditions where θ_0 will have a clear physical interpretation. For example, in the calorimetric setup θ_0 can be viewed as the minimum angle between the photon and the charged particle when they are detected separately (at smaller angles the two particles form a single cluster in the calorimeter, so that they are detected as a single particle with the total energy).

For definiteness, in the calculations we have considered only emission from the electron line; the contribution of positron emission is identical. The sum of the contributions of the two kinematics (some details of the calculations are given in Appendix C) has the form

$$\Sigma^{HH}=\Sigma_{HH}=\frac{1}{4}\left(\frac{\alpha}{\pi}\right)^2\int_1^{\rho^2}dz\, z^{-2}(1-\Pi(-zQ_1^2))^{-2}$$
$$\times\int_{x_c}^{1-2\Delta}dx\int_\Delta^{1-x-\Delta}dx_1\,\frac{I^{HH}L}{x_1(1-x-x_1)(1-x_1)^2},$$
$$I^{HH}=A\Theta(x^2\rho^2-z)+B+C\Theta((1-x_1)^2\rho^2-z), \qquad (46)$$

where

$$A=\gamma\beta\left(\frac{L}{2}+\ln\frac{(\rho^2x^2-z)^2}{x^2(\rho^2x(1-x_1)-z)^2}\right)+(x^2+(1-x_1)^4)\ln\frac{(1-x_1)^2(1-x-x_1)}{xx_1}+\gamma_A,$$

$$B=\gamma\beta\left(\frac{L}{2}+\ln\left|\frac{x^2(z-1)(\rho^2-z)(z-x^2)(z-(1-x_1)^2)^2(\rho^2x(1-x_1)-z)^2}{(\rho^2x^2-z)(z-(1-x_1))^2(\rho^2(1-x_1)^2-z)^2(z-x(1-x_1))^2}\right|\right)+(x^2+(1-x_1)^4)\ln\frac{(1-x_1)^2x_1}{x(1-x-x_1)}+\delta_B,$$

$$C=\gamma\beta\left(L+2\ln\left|\frac{x(\rho^2(1-x_1)^2-z)^2}{(1-x_1)^2(\rho^2x(1-x_1)-z)(\rho^2(1-x_1)-z)}\right|\right)-2(1-x_1)\beta-2x(1-x_1)\gamma,$$

$$\gamma=1+(1-x_1)^2,\quad \beta=x^2+(1-x_1)^2,$$

$$\gamma_A=xx_1(1-x-x_1)-x_1^2(1-x-x_1)^2-2(1-x_1)\beta,$$

$$\delta_B=xx_1(1-x-x_1)-x_1^2(1-x-x_1)^2-2x(1-x_1)\gamma.$$

It can be verified that the combination

$$\left(\frac{\alpha}{\pi}\right)^2\int_1^{\rho^2}\frac{dz}{z^2}(1-\Pi(-zQ_1^2))^{-2}r_{S+V}^{\gamma\gamma}+\Sigma^{H(S+V)}+\Sigma^{HH},$$
$$\left(\frac{\alpha}{\pi}\right)^2\int_1^{\rho^2}\frac{dz}{z^2}(1-\Pi(-zQ_1^2))^{-2}r_{S+V\gamma}^{\gamma}+\Sigma_{S+V}^{H}+\Sigma_H^{S+V}+\Sigma_H^H \qquad (47)$$

is independent of Δ for $\Delta\to 0$ (see Appendix D).

The complete expression for $\Sigma^{2\gamma}$ describing the contributions to (2) from the emission of two real and virtual photons is given by the sum

$$\Sigma^{2\gamma}=\Sigma_{S+V}^{\gamma\gamma}+2\Sigma^{H(V+S)}+2\Sigma_{S+V}^{H}+\Sigma_H^H+2\Sigma^{HH}$$
$$=\Sigma^{\gamma\gamma}+\Sigma_\gamma^\gamma+\phi^{\gamma\gamma}+\phi_\gamma^\gamma, \qquad (48)$$

which is independent of the auxiliary parameter Δ.

The contributions in the leading-log approximation (see Appendix E) have the form

$$\Sigma^{\gamma\gamma}=\frac{1}{2}\left(\frac{\alpha}{\pi}\right)^2\int_1^{\rho^2}L^2dz\,z^{-2}(1-\Pi(-Q_1^2z))^{-2}$$
$$\times\int_{x_c}^1 dx\left\{\frac{1}{2}P^{(2)}(x)[\Theta(x^2\rho^2-z)+1]\right.$$
$$\left.+\int_x^1\frac{dt}{t}P(t)P\left(\frac{x}{t}\right)\Theta(t^2\rho^2-z)\right\}, \qquad (49)$$

$$P^{(2)}(x)=\int_x^1\frac{dt}{t}P(t)P\left(\frac{x}{t}\right)=\lim_{\Delta\to 0}\left\{\left[\left(2\ln\Delta+\frac{3}{2}\right)^2\right.\right.$$
$$\left.-4\zeta_2\right]\delta(1-x)+2\left[\frac{1+x^2}{1-x}\left(2\ln(1-x)-\ln x\right.\right.$$
$$\left.\left.\left.+\frac{3}{2}\right)+\frac{1}{2}(1+x)\ln x-1+x\right]\Theta(1-x-\Delta)\right\}, \qquad (50)$$

$$\Sigma_{\gamma}^{\gamma}=\frac{1}{4}\left(\frac{\alpha}{\pi}\right)^2\int_0^{\infty}L^2dz\,z^{-2}(1-\Pi(-Q_1^2z))^{-2}$$
$$\times\int_{x_c}^1dx_1\int_{x_e/x_1}^1dx_2P(x_1)P(x_2)[\Theta(z-1)\Theta(\rho^2$$
$$-z)+\Theta(z-x_1^2)\Theta(x_1^2\rho^2-z)][\Theta(z-1)\Theta(\rho^2-z)$$
$$+\Theta(z-x_2^2)\Theta(x_2^2\rho^2-z)]. \qquad (51)$$

We see that the leading contributions to $\Sigma^{2\gamma}$ are represented in terms of the kernels of the structure-function evolution equations.

The functions $\phi^{\gamma\gamma}$ and ϕ_{γ}^{γ} in (48) collect the nonleading contributions, which cannot be obtained by the structure-function technique.[11–14] Their explicit form can be determined by comparing the results in the logarithmic and leading-log approximations, given below.

5. PRODUCTION OF e^+e^- PAIRS IN BHABHA SCATTERING

Let us now turn to the $\mathscr{O}(\alpha^2)$ corrections associated with e^+e^- pair production in small-angle Bhabha scattering. We shall include the contributions of virtual, soft, and hard real pairs. In the case of hard-pair production we need to consider both the collinear and the semicollinear kinematics. We shall assume that in the pair-production process

$$e^-(p_1)+e^+(p_2)\to e^-(q_1)+e^+(q_2)+e^-(p_-)$$
$$+e^+(p_+)$$

an electron and a positron with momenta q_1 and q_2, respectively, are detected. The fact that the two pairs of particles in the final state are identical is taken into account by studying the corresponding Feynman diagrams.

We define the region of collinear kinematics as the region of the phase space of the final particles in which the electron and positron of the undetected pair move inside a narrow cone about the direction of the momentum of one of the charged initial or detected final particles:

$$\widehat{\mathbf{p}_+\mathbf{p}_-}\sim\widehat{\mathbf{p}_-\mathbf{p}_i}\sim\widehat{\mathbf{p}_+\mathbf{p}_i}<\theta_0\ll 1,$$
$$\varepsilon\theta_0/m\gg 1,\quad \mathbf{p}_i=\mathbf{p}_1,\mathbf{p}_2,\mathbf{q}_1,\mathbf{q}_2. \qquad (52)$$

The contribution of the collinear kinematics contains terms of order $(\alpha L/\pi)^2$ and $(\alpha/\pi)^2L$. In the semicollinear kinematics only one of the conditions (52) on the angles is satisfied:

$$\widehat{\mathbf{p}_+\mathbf{p}_-}<\theta_0,\quad \widehat{\mathbf{p}_\pm\mathbf{p}_i}>\theta_0;\ \text{or}\ \widehat{\mathbf{p}_-\mathbf{p}_i}<\theta_0,\quad \widehat{\mathbf{p}_+\mathbf{p}_i}>\theta_0;$$
$$\text{or}\ \widehat{\mathbf{p}_-\mathbf{p}_i}>\theta_0,\quad \widehat{\mathbf{p}_+\mathbf{p}_i}<\theta_0.$$

The contribution of the semicollinear kinematics contains terms of the form

$$\left(\frac{\alpha}{\pi}\right)^2L\ln\frac{\theta_0}{\theta},\quad \left(\frac{\alpha}{\pi}\right)^2L,$$

where $\theta=\widehat{\mathbf{p}_-\mathbf{q}_1}$ is the electron scattering angle. The auxiliary parameter θ_0 cancels in the sum of the contributions of the collinear and semicollinear kinematics. As above, we systematically discard terms which do not contain the large logarithm L.

We have limited our study to the case of electron–positron pair production. The effects of the production of other pairs ($\mu^+\mu^-$, $\pi^+\pi^-$, and so on) are at least an order of magnitude (see Ref. 9) smaller than the ones studied here, and they can be dropped in view of the numerical results presented below.

Pair production in collisions of high-energy leptons has received a great deal of attention (see Ref. 9 and references therein). In particular, it has been shown that the total cross section contains contributions proportional to the cube of the large logarithm originating from the two-photon mechanism of pair production with small invariant mass of the pair. Taking into account the fact that in this case the scattered electron and positron move at very small angles ($\sim m/\varepsilon$) relative to the beam axes, it can be verified that such events cannot be detected at LEP I.

Taking into account all the possible mechanisms of (singlet and nonsinglet) pair production plus the LEP I experimental conditions and the fact that the particles in the final state are identical, it is possible to construct 36 Feynman diagrams describing the production of real e^+e^- pairs at tree level. In the case of small-angle Bhabha scattering only some of these graphs contribute to the correction to the cross section, namely, those of the scatterer type. Moreover, direct calculations show that the contributions from interference of the amplitudes describing pair emission along the direction of the electron beam with the amplitudes describing pair emission along the positron beam cancel. This is a manifestation of the above-mentioned cancellation of the contributions originating in up–down interference.

The cubes of the large logarithm cancel in the sum of the contributions from virtual-pair emission (owing to the vacuum-polarization insertion in the virtual-photon propagator) and from the emission of real soft pairs, but the auxiliary parameter $\Delta=\delta\varepsilon/\varepsilon$ ($m_e\ll\delta\varepsilon\ll\varepsilon$, where $\delta\varepsilon$ is the total en-

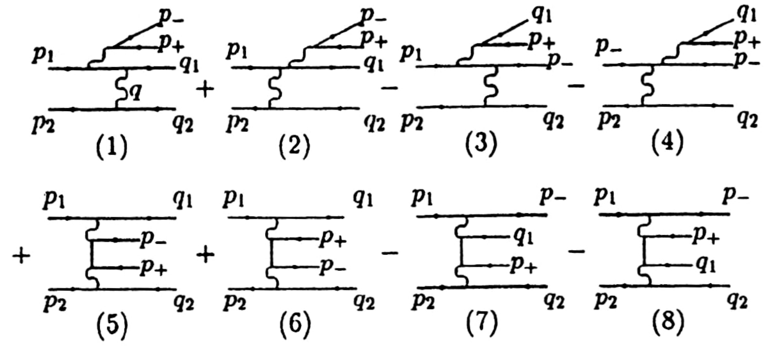

FIG. 1. Feynman diagrams giving logarithmically enhanced contributions when the pair moves along the directions of the final or initial electron.

ergy of the components of the soft pair) remains. The Δ dependence disappears in the full sum after addition of the contribution from real hard pairs. Before summing it is necessary to integrate the contribution of hard pairs over the energy fractions of the pair components and over the energy fractions of the detected electron and positron:

$$\Delta=\frac{\delta\varepsilon}{\varepsilon}<x_1+x_2,\quad x_c<x=1-x_1-x_2<1-\Delta,$$

$$x_1=\frac{\varepsilon_+}{\varepsilon},\quad x_2=\frac{\varepsilon_-}{\varepsilon},\quad x=\frac{q_1^0}{\varepsilon},$$

where $\varepsilon_\pm$ are the energies of the positron and electron of the created pair.

5.1. Collinear kinematic regions

Altogether, there are four regions of collinear kinematics: a pair can move along the momentum of the initial electron (positron) or along the momentum of the final detected electron (positron). For definiteness, we shall consider the case of motion of the pair only along the directions of the initial and final electron. To include the motion along the positron directions in the case of symmetric detectors we simply multiply the result by two.

For pair emission along the direction of the initial electron it is convenient to decompose the particle momenta into longitudinal and transverse components:

$$p_+=x_1p_1+\mathbf{p}_+^\perp,\quad p_-=x_2p_1+\mathbf{p}_-^\perp,\quad q_1=xp_1+\mathbf{q}_1^\perp,$$

$$x=1-x_1-x_2,\quad q_2\approx p_2,\quad \mathbf{p}_+^\perp+\mathbf{p}_-^\perp+\mathbf{q}_1^\perp=0,$$

where $\mathbf{p}_i^\perp$ are the two-dimensional components of the final particles perpendicular to the direction of the initial electron beam. We introduce dimensionless quantities related to the kinematic invariants:

$$z_i=\left(\frac{\varepsilon\theta_i}{m}\right)^2,\quad z_1=\left(\frac{\mathbf{p}_-^\perp}{m}\right)^2,\quad z_2=\left(\frac{\mathbf{p}_+^\perp}{m}\right)^2,$$

$$0<z_i<\left(\frac{\varepsilon\theta_0}{m}\right)^2\gg 1,$$

$$A=\frac{(p_++p_-)^2}{m^2}=(x_1x_2)^{-1}[(1-x)^2+x_1^2x_2^2(z_1+z_2-2\sqrt{z_1z_2}\cos\phi)],$$

$$A_1=\frac{2p_1p_-}{m^2}=x_2^{-1}[1+x_2^2+x_2^2z_2],$$

$$A_2=\frac{2p_1p_+}{m^2}=x_1^{-1}[1+x_1^2+x_1^2z_1],$$

$$C=\frac{(p_1-p_-)^2}{m^2}=2-A_1,$$

$$D=\frac{(p_1-q_1)^2}{m^2}-1=A-A_1-A_2,$$

where ϕ is the azimuthal angle between the planes $(\mathbf{p}_1\mathbf{p}_+^\perp)$ and $(\mathbf{p}_1\mathbf{p}_-^\perp)$. Keeping in the matrix element summed over spin states only terms giving nonzero contributions for $\theta_0\to 0$, we find that only eight of the 36 Feynman diagrams are important. These are shown in Fig. 1, where the sign in front of a graph includes the Fermi–Dirac statistics for interchange of identical fermions.

The result for this collinear kinematics has a factorized form, which is consistent with the known factorization theorem:[26]

$$\sum_{\text{spins}}|M|^2\Big|_{p_+,p_-\parallel p_1}=\sum_{\text{spins}}|M_0|^2 2^7\pi^2\alpha^2\frac{I}{m^4},$$

where one of the cofactors corresponds to the Born matrix element (without pair production):

$$\sum_{\text{spin}}|M_0|^2=2^7\pi^2\alpha^2\left(\frac{s^4+t^4+u^4}{s^2t^2}\right),$$

$$s=2p_1p_2x,\quad t=-Q^2x,\quad u=-s-t,$$

and the quantity I, referred to as the collinear factor, coincides with the expression obtained in Ref. 22. In our kinematic variables it is written as

$$I=(1-x_2)^{-2}\left(\frac{A(1-x_2)+Dx_2}{DC}\right)^2+(1-x)^{-2}\left(\frac{C(1-x)-Dx_2}{AD}\right)^2+\frac{1}{2xAD}\left[\frac{2(1-x_2)^2-(1-x)^2}{1-x}+\frac{x_1x-x_2}{1-x_2}+3(x_2-x)\right]+\frac{1}{2xCD}\left[\frac{(1-x_2)^2-2(1-x)^2}{1-x_2}+\frac{x-x_1x_2}{1-x}\right.$$

$$+3(x_2-x)\Big] + \frac{x_2(x^2+x_2^2)}{2x(1-x_2)(1-x)AC} + \frac{3x}{D^2} + \frac{2C}{AD^2}$$
$$+\frac{2A}{CD^2} + \frac{2(1-x_2)}{xA^2D} - \frac{4C}{xA^2D^2} - \frac{4A}{D^2C^2}$$
$$+\frac{1}{DC^2}\left[\frac{(x_1-x)(1+x_2)}{x(1-x_2)} - 2\frac{1-x}{x}\right].$$

We transform the phase space of the final particles to the form

$$d\Gamma = \frac{d^3\mathbf{q}_1 d^3\mathbf{q}_2}{(2\pi)^6 2q_1^0 2q_2^0}(2\pi)^4\delta^{(4)}(p_1x+p_2-q_1-q_2)m^4 2^{-8}\pi^{-4}x_1x_2dx_1dx_2dz_1dz_2\frac{d\phi}{2\pi}$$

and integrate over the variables of the created pair (the details can be found in Ref. 23):

$$\bar{I} = \int_0^{2\pi}\frac{d\phi}{2\pi}\int_0^{z_0}dz_1\int_0^{z_0}dz_2 I = \frac{L_0}{2xx_1x_2}\left\{D_1\left(L_0 + 2\ln\frac{x_1x_2}{x}\right) + D_2\ln\frac{(1-x_2)(1-x)}{xx_2} + D_3\right\},$$

$$L_0 = \ln\left(\frac{\varepsilon\theta_0}{m}\right)^2,$$

$$D_1 = 2xx_1x_2\left(\frac{1}{(1-x)^4} + \frac{1}{(1-x_2)^4}\right) - \frac{(1-x_2)^2}{(1-x)^2} - \frac{(1-x)^2}{(1-x_2)^2} + 1 + \frac{(x+x_2)^2}{2(1-x)(1-x_2)}$$
$$+\frac{3(x_2-x)^2}{2(1-x)(1-x_2)} - \frac{x^2+x_2^2}{(1-x)(1-x_2)} - 2xx_2\left(\frac{1}{(1-x)^2} + \frac{1}{(1-x_2)^2}\right),$$

$$D_2 = \frac{2(x^2+x_2^2)}{(1-x)(1-x_2)},$$

$$D_3 = \frac{2xx_1x_2}{(1-x_2)^2}\left(-\frac{8}{(1-x_2)^2} + \frac{(1-x)^2}{xx_1x_2}\right)$$
$$+\frac{2xx_1x_2}{(1-x)^2}\left[\frac{x_2}{xx_1} + \frac{2(x_1-x_2)}{xx_1(1-x)} - \frac{8}{(1-x)^2} + \frac{1}{xx_1x_2} - \frac{4}{x(1-x)}\right] + 6 + 4x\left[\frac{x_2-x_1}{(1-x)^2} - \frac{x_1}{x(1-x)}\right]$$
$$+\frac{4(xx_2-x_1)}{(1-x_2)^2} - \frac{4(1-x_2)x_1x_2}{(1-x)^3} + \frac{8xx_1x_2^2}{(1-x)^4}$$
$$-\frac{xx_2^2}{(1-x_2)^4} + \frac{x_2}{(1-x_2)^2}\left[4(1-x) + \frac{2(x-x_1)(1+x_2)}{1-x_2}\right].$$

Performing the analogous operations in the case where the pair moves in the direction of the scattered electron, integrating the sum over the energy fractions of the pair components, and, finally, adding the other two collinear regions where the pair moves along the direction of the initial or final positron, we obtain

$$d\sigma_{\text{coll}} = \frac{\alpha^4 dx}{\pi Q_1^2}\int_1^{\rho^2}\frac{dz}{z^2}L\left\{R_0(x)\left(L + 2\ln\frac{\eta^2}{z}\right)(1+\Theta) + 4R_0(x)\ln x + 2\Theta f(x) + 2f_1(x)\right\},$$

$$\eta = \frac{\theta_0}{\theta_{\min}}, \quad \Theta \equiv \Theta(x^2\rho^2 - z),$$

$$R_0(x) = \frac{2}{3}\frac{1+x^2}{1-x} + \frac{(1-x)}{3x}(4+7x+4x^2) + 2(1+x)\ln x,$$

$$f(x) = -\frac{107}{9} + \frac{136}{9}x - \frac{2}{3}x^2 - \frac{4}{3x} - \frac{20}{9(1-x)} + \frac{2}{3}\times\left[-4x^2 - 5x + 1 + \frac{4}{x(1-x)}\right]\ln(1-x) + \frac{1}{3}\left[8x^2 + 5x - 7 - \frac{13}{1-x}\right]\ln x - \frac{2}{1-x}\ln^2 x + 4(1+x)\ln x\ln(1-x) - \frac{2(3x^2-1)}{1-x}\mathrm{Li}_2(1-x),$$

$$f_1(x) = -x\,\mathrm{Re}\,f\left(\frac{1}{x}\right) = -\frac{116}{9} + \frac{127}{9}x + \frac{4}{3}x^2 + \frac{2}{3x} - \frac{20}{9(1-x)} + \frac{2}{3}\left[-4x^2 - 5x + 1 + \frac{4}{x(1-x)}\right]\ln(1-x) + \frac{1}{3}\left[8x^2 - 10x - 10 + \frac{5}{1-x}\right]\ln x - (1+x)\ln^2 x + 4(1+x)\ln x\ln(1-x) - \frac{2(x^2-3)}{1-x}\mathrm{Li}_2(1-x),$$

$$\mathrm{Li}_2(x) \equiv -\int_0^x\frac{dy}{y}\ln(1-y), \quad Q_1 = \varepsilon\theta_{\min},$$

$$L = \ln\frac{zQ_1^2}{m^2}, \tag{53}$$

5.2. Semicollinear kinematic regions

Again we restrict ourselves to the case of pair emission from an electron line. There are three different semicollinear kinematic regions which contribute for the accuracy to which we are working. The first region includes events with very small invariant mass of the created pair:

$$4m^2 \ll (p_+ + p_-)^2 \ll |q^2|,$$

where the two particles of this pair do not fall into the narrow cones described above and specified by the same angle θ_0 about the momenta of the initial and final electrons. We shall denote this region by $\mathbf{p}_+ \| \mathbf{p}_-$. Only graphs (1) and (2) of Fig. 1 contribute in this case, owing to the smallness of the denominator of the virtual photon producing the pair.

The second semicollinear region includes events in which the invariant mass of the system of created positron and scattered electron is small: $4m^2 \ll (p_+ + q_1)^2 \ll |q^2|$, where the created positron must not fall into the narrow cone about the momentum of the initial electron. We denote this region by $\mathbf{p}_+ \| \mathbf{q}_1$ and note that only graphs (3) and (4) of Fig. 1 contribute to it.

The third semicollinear region includes events in which the electron of the created pair moves inside the narrow cone along the momentum of the initial electron, and the positron does not. We shall denote this region by $\mathbf{p}_- \| \mathbf{p}_1$. Here only graphs (7) and (8) of Fig. 1 are important.

We write the differential cross section for the pair-production process as

$$d\sigma = \frac{\alpha^4}{8\pi^4 s^2} \frac{|M|^2}{q^4} \frac{dx_1 dx_2 dx}{x_1 x_2 x} d^2\mathbf{p}_+^\perp d^2\mathbf{p}_-^\perp d^2\mathbf{q}_1^\perp d^2\mathbf{q}_2^\perp \delta(1 - x_1 - x_2 - x)\, \delta^{(2)}(\mathbf{p}_+^\perp + \mathbf{p}_-^\perp + \mathbf{q}_1^\perp + \mathbf{q}_2^\perp),$$

$$|M|^2 = -L_{\lambda\rho} p_{2\lambda} p_{2\rho}, \tag{54}$$

where x_1 (x_2), x and $\mathbf{p}_+^\perp$ ($\mathbf{p}_-^\perp$), $\mathbf{q}_1^\perp$ are the energy fractions and transverse momenta of the created electron (positron) and scattered electron, respectively; $s = (p_1 + p_2)^2$ and $q^2 = -Q^2 = (p_2 - q_2)^2 = -\varepsilon^2\theta^2$ are the square of the total energy in the c.m. frame and the squared momentum transfer. The leptonic tensor $L_{\lambda\rho}$ has a different form in each of the three semicollinear regions.

Let us consider the region $\mathbf{p}_+ \| \mathbf{p}_-$. In this region we can use the leptonic tensor obtained in Ref. 22. Keeping only the important terms, we write it as

$$\frac{P^4}{8} L_{\lambda\rho} = \frac{4P^2q^2}{(1)(2)} [-(p_1p_1)_{\lambda\rho} - (q_1q_1)_{\lambda\rho} + (p_1q_1)_{\lambda\rho}] - 4(p_+p_-)_{\lambda\rho}\left(1 - \frac{q^2P^2}{(1)(2)}\right) - \frac{4}{(1)} [q^2(p_1q_1)_{\lambda\rho} - 2(p_1p_+)(q_1p_-)_{\lambda\rho} - 2(p_1p_-)(q_1p_1)_{\lambda\rho}] - \frac{4}{(2)} [P^2(p_1q_1)_{\lambda\rho} - 2(p_+q_1)(p_1p_-)_{\lambda\rho} - 2(p_-q_1)(p_1p_+)_{\lambda\rho}] - \frac{32(p_1p_+)(p_1p_-)}{(1)^2}(q_1q_1)_{\lambda\rho} - \frac{32(q_1p_+)(q_1p_-)}{(2)^2}(p_1p_1)_{\lambda\rho} + \frac{8(p_1q_1)_{\lambda\rho}}{(1)(2)} [P^2(p_1q_1) - 2(p_1p_+)(p_-q_1) - 2(p_1p_-)(q_1p_+)], \tag{55}$$

where

$$P = p_+ + p_-, \quad (aa)_{\lambda\rho} = a_\lambda a_\rho,$$

$$(ab)_{\lambda\rho} = a_\lambda b_\rho + a_\rho b_\lambda,$$

$$q = p_1 - q_1 - P, \quad (1) = (p_1 - P)^2 - m^2,$$

$$(2) = (p_1 - q)^2 - m^2.$$

After some algebra, the expression for the squared matrix element entering into (54) can be written as

$$\frac{1}{q^4}|M|^2 = -\frac{2s^2}{q^4P^4}\left\{-\frac{4P^2q^2}{(1)(2)}[(1-x_1)^2 + (1-x_2)^2] + \frac{128}{(1)^2(2)^2}[(q_1p)(p_+p_1) - x(p_1p) \times (q_1p_+)]^2\right\},$$

where $p = p_- - x_2 p_+ / x_1$ and $(\mathbf{q}_2^\perp)^2 = -q^2$. In this region we can use the following relations:

$$(1) = -\frac{1-x}{x_1} 2(p_1p_+), \quad (2) = \frac{1-x}{x_1} 2(q_1p_+).$$

It is useful to represent all the invariants in terms of Sudakov variables (energy fractions and transverse components of momentum):

$$q_1^2 = \frac{1}{x_1x_2}((\mathbf{p}^\perp)^2 + m^2(1-x)^2),$$

$$2(q_1p_+) = \frac{1}{xx_1}(x\mathbf{p}_+^\perp - x_1\mathbf{q}_1^\perp)^2,$$

$$2(p_1p_+) = \frac{1}{x_1}(\mathbf{p}_+^\perp)^2, \quad 2(p_1p) = \frac{2}{x_1^2}\mathbf{p}^\perp\mathbf{p}_+^\perp,$$

$$2(q_1p) = \frac{2}{x_1^2}(\mathbf{p}^\perp[x\mathbf{p}_+^\perp - x_1\mathbf{q}_1^\perp]),$$

$$\mathbf{p}^\perp = x_1\mathbf{p}_-^\perp - x_2\mathbf{p}_+^\perp.$$

The large logarithm which we are trying to extract appears in the integration over $\mathbf{p}^\perp$. To perform this integration we use the relation

$$\delta^{(2)}(\mathbf{p}_+^\perp + \mathbf{p}_-^\perp + \mathbf{q}_1^\perp + \mathbf{q}_2^\perp) d^2\mathbf{p}_+^\perp d^2\mathbf{p}_-^\perp = \frac{1}{(1-x)^2} d^2\mathbf{p}^\perp,$$

which is true in the region $\mathbf{p}_+ \| \mathbf{p}_-$. Integrating, we obtain the following contribution to the cross section for small-angle Bhabha scattering from this region:

$$d\sigma_{\mathbf{p}_+\|\mathbf{p}_-} = \frac{\alpha^4}{\pi} L dx dx_2 \frac{d(\mathbf{q}_2^\perp)^2}{(\mathbf{q}_2^\perp)^2} \frac{d(\mathbf{q}_1^\perp)^2}{(\mathbf{q}_1^\perp + \mathbf{q}_2^\perp)^2} \times \frac{d\phi}{2\pi} \frac{1}{(\mathbf{q}_1^\perp + x\mathbf{q}_2^\perp)^2}\left[(1-x_1)^2 + (1-x_2)^2 - \frac{4xx_1x_2}{(1-x)^2}\right],$$

where ϕ is the angle between the two-vectors $\mathbf{q}_1^\perp$ and $\mathbf{q}_2^\perp$.

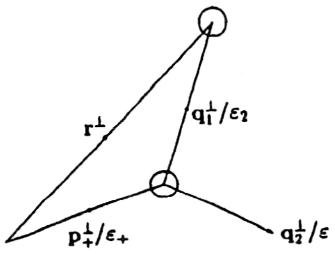

FIG. 2. Kinematics of an event with pair production in the plane perpendicular to the beam axes for the semicollinear region $\mathbf{p}_+ \| \mathbf{p}_-$.

At this stage it is necessary to use the restrictions on $\mathbf{q}_1^\perp$ and $\mathbf{q}_2^\perp$. These restrictions arise if we discard the part of the phase space corresponding to the case of collinear kinematics already considered. That is, we must exclude the narrow cones about the momenta of the initial and final electrons.

The event kinematics is shown in Fig. 2, where the circles of radius θ_0 around the points corresponding to the directions of the momenta of the initial and final electrons bound the forbidden collinear regions. The exclusion of these regions leads to the following restrictions:

$$\left|\frac{\mathbf{p}_+^\perp}{\varepsilon_+}\right| > \theta_0, \quad |\mathbf{r}^\perp| = \left|\frac{\mathbf{p}_+^\perp}{\varepsilon_+} - \frac{\mathbf{q}_1^\perp}{\varepsilon_2}\right| > \theta_0, \tag{56}$$

where ε_+ and ε_2 are the energies of the created positron and scattered electron, respectively. To eliminate $\mathbf{p}_+^\perp$ we use the law of conservation of transverse momentum, which holds in this region:

$$\mathbf{q}_1^\perp + \mathbf{q}_2^\perp + \frac{1-x}{x_1}\,\mathbf{p}_+^\perp = 0.$$

It is useful to introduce the dimensionless variables $z_{1,2} = (\mathbf{q}_{1,2}^\perp)^2/(\varepsilon\theta_{\min})^2$, where $\theta_{\min}$ is the minimum angle of detection of the scattered electron and positron. The conditions (56) are rewritten as

$$\begin{cases} 1 > \cos\phi > -1 + \dfrac{\eta^2(1-x)^2 - (\sqrt{z_1} - \sqrt{z_2})^2}{2\sqrt{z_1 z_2}}, \\ |\sqrt{z_1} - \sqrt{z_2}| < \eta(1-x), \\ 1 > \cos\phi > -1, \quad |\sqrt{z_1} - \sqrt{z_2}| > \eta(1-x), \quad \eta = \theta_0/\theta_{\min}, \end{cases} \tag{57}$$

$$\begin{cases} 1 > \cos\phi > -1 + \dfrac{\eta^2 x^2(1-x)^2 - (\sqrt{z_1} - x\sqrt{z_2})^2}{2x\sqrt{z_1 z_2}} \\ |\sqrt{z_1} - x\sqrt{z_2}| < \eta x(1-x), \\ 1 > \cos\phi > -1, \quad |\sqrt{z_1} - x\sqrt{z_2}| > \eta x(1-x). \end{cases} \tag{58}$$

The conditions (57) eliminate pair emission in the narrow cone about the direction of the initial electron, and the conditions (58) eliminate that of the scattered electron. We impose the following condition on the auxiliary parameter θ_0:

$$\theta_0 \gg \frac{m}{\varepsilon} \approx 10^{-5},$$

and the experimental limits are of order $\theta_{\min} \sim 10^{-2}$. This allows us to assume that $\eta \ll 1$. The procedure for integrating the differential cross section with these conditions is described in detail in Ref. 23. Here we give the contribution to the cross section from this kinematic region with the condition that only those scattered electrons whose energy fractions x exceed a given value x_c are detected:

$$\begin{aligned} \sigma_{\mathbf{p}_+\|\mathbf{p}_-} = {} & \frac{\alpha^4}{\pi Q_1^2}\mathscr{L}\int_1^{\rho^2}\frac{dz}{z^2}\int_{x_c}^{1-\Delta}dx\int_0^{1-x}dx_2 \\ & \times\left[\frac{(1-x_1)^2+(1-x_2)^2}{(1-x)^2} - \frac{4xx_1x_2}{(1-x)^2}\right]\Bigg\{(1 \\ & +\Theta)\ln\frac{z}{\eta^2} + \Theta\ln\frac{(x^2\rho^2-z)^2}{x^2(x\rho^2-z)^2} \\ & + \ln\left|\frac{(z-x^2)(\rho^2-z)(z-1)}{(z-x)^2(z-x^2\rho^2)}\right|\Bigg\}, \end{aligned}$$

$$\mathscr{L} = \ln\frac{\varepsilon^2\theta_{\min}^2}{m^2}, \tag{59}$$

where $\Theta \equiv \Theta(x^2\rho^2 - z)$, $z \equiv z_2$. The auxiliary parameter Δ entering into (59) specifies the minimum energy of the created hard pair: $2m/\varepsilon \ll \Delta \ll 1$. We note that we have replaced L by $\mathscr{L}$, since we do not distinguish them at the one-logarithm level.

Let us now consider the region $\mathbf{p}_+ \| \mathbf{q}_1$. As already noted, in this region only graphs (3) and (4) of Fig. 1 give a logarithmically enhanced contribution. The leptonic tensor for this case can be obtained from (55) by means of the replacement $p_- \leftrightarrow q_1$. The square of the matrix element is written as

$$\begin{aligned} |M|^2_{\mathbf{p}_+\|\mathbf{q}_i} = {} & -\frac{4s^2}{q_1'^2\mathbf{q}_2^{\perp 2}}\frac{1}{(1')(2)}\Bigg\{(1-x_1)^2+(1-x_2)^2 \\ & + \frac{32}{q_1'^2\mathbf{q}_2^{\perp 2}}\frac{1}{(1')(2)}[(p_1p_+)(p_-p') \\ & - x_2(p_-p_+)(p_1p')]^2\Bigg\}, \end{aligned}$$

where

$$p' = q_1 - p_+x/x_1, \quad q_1'^2 = (q_1 + p_+)^2,$$

$$(2) = 2(p_+p_-)(1-x_2)/x_1,$$

$$(1') = -2(p_1p_+)(1-x_2)/x_1.$$

The integration over $(\mathbf{p}_1^\perp)^2$ and $(\mathbf{p}_-^\perp)^2$ can be performed as in the preceding case, and the contribution to the differential cross section can be written as

$$\begin{aligned} d\sigma_{\mathbf{p}_+\|\mathbf{q}_1} = {} & \frac{\alpha^4}{\pi}L\,dx\,dx_2\,\frac{d(\mathbf{q}_2^\perp)^2}{(\mathbf{q}_2^\perp)^2}\frac{d(\mathbf{q}_1^\perp)^2}{(\mathbf{q}_1^\perp)^2}\frac{d\phi}{2\pi} \\ & \times\frac{1}{(\mathbf{q}_1^\perp + x\mathbf{q}_2^\perp)^2}\frac{x^2}{(1-x_2)^2}\Bigg[(1-x)^2+(1-x_1)^2 \\ & - \frac{4xx_1x_2}{(1-x_2)^2}\Bigg]. \end{aligned} \tag{60}$$

The restrictions on the phase space reflecting the exclusion of the collinear region of motion of the created pair inside the narrow cone about the momentum of the scattered electron lead to the inequality

$$\left|\frac{\mathbf{p}_-^\perp}{\varepsilon_-}-\frac{\mathbf{q}_1^\perp}{\varepsilon_2}\right|>\theta_0. \tag{61}$$

We shall eliminate $\mathbf{p}_-^\perp$ from (61), using the conservation of transverse momentum in the form valid in this kinematic region: $\mathbf{p}_-^\perp+\mathbf{q}_2^\perp+\mathbf{q}_1^\perp(1-x_2)/x=0$. The condition (61) can be rewritten in terms of the dimensionless variables z_1, z_2 and the angle ϕ as

$$\begin{cases} 1>\cos\phi>-1+\dfrac{\eta^2x^2x_2^2-(\sqrt{z_1}-x\sqrt{z_2})^2}{2x\sqrt{z_1z_2}}, \\ |\sqrt{z_1}-x\sqrt{z_2}|<\eta x x_2, \\ 1>\cos\phi>-1,\quad |\sqrt{z_1}-x\sqrt{z_2}|>\eta x x_2. \end{cases} \tag{62}$$

Integration of the differential cross section (60) over the region (62) gives

$$\sigma_{\mathbf{p}_+\|\mathbf{q}_1}=\frac{\alpha^4}{\pi Q_1^2}\mathscr{L}\int_1^{\rho^2}\frac{dz}{z^2}\int_{x_c}^{1-\Delta}dx\int_0^{1-x}dx_2 \times\left[\frac{(1-x)^2+(1-x_1)^2}{(1-x_2)^2}-\frac{4xx_1x_2}{(1-x_2)^4}\right]\left\{\ln\frac{z}{\eta^2}+\ln\frac{(\rho^2-z)(z-1)}{x_2^2\rho^2}\right\}. \tag{63}$$

Let us now consider the third semicollinear kinematic region $\mathbf{p}_-\|\mathbf{p}_1$, in which graphs (7) and (8) of Fig. 2 are important. The leptonic tensor can be obtained from Eq. (55) by the replacement $p_1\leftrightarrow -p_+$. The squared modulus of the matrix element has the form

$$|M|^2_{\mathbf{p}_-\|\mathbf{p}_1}=-\frac{4s^2}{q_2'^2(\mathbf{q}_2^\perp)^2}\cdot\frac{1}{(1)(2')}\left\{(1-x)^2+(1-x_1)^2+\frac{32}{q_2'^2(\mathbf{q}_2^\perp)^2}\cdot\frac{1}{(1)(2')}[x_1(p_1\tilde{p})(p_1p_+)+x(p_+\tilde{p})(q_1p_1)]^2\right\},$$

where

$$\tilde{p}=p_--x_2p_1,\quad q_2'^2=(p_1-p_-)^2,$$

$$(2')=-2(p_1q_1)(1-x_2),\quad (1)=-2(p_1p_+)(1-x_2).$$

Integration over $(\mathbf{p}_+^\perp)^2$ and $(\mathbf{p}_-^\perp)^2$ leads to the differential cross section

$$d\sigma_{\mathbf{p}_-\|\mathbf{p}_1}=\frac{\alpha}{4\pi}Ldxdx_2\frac{d(\mathbf{q}_2^\perp)^2}{(\mathbf{q}_2^\perp)^2}\frac{d(\mathbf{q}_1^\perp)^2}{(\mathbf{q}_1^\perp)^2}\frac{d\phi}{2\pi}\frac{1}{(\mathbf{q}_1^\perp+\mathbf{q}_2^\perp)^2} \times\left[\frac{(1-x)^2+(1-x_1)^2}{(1-x_2)^2}-\frac{4xx_1x_2}{(1-x_2)^4}\right]. \tag{64}$$

The restriction corresponding to exclusion of the collinear kinematic region in which the created pair moves inside a narrow cone about the momentum of the initial electron has the form

$$\frac{|\mathbf{p}_+^\perp|}{\varepsilon_1}>\theta_0,\quad \mathbf{p}_+^\perp+\mathbf{q}_1^\perp+\mathbf{q}_2^\perp=0,$$

or

$$\begin{cases} 1>\cos\phi>-1+\dfrac{\eta^2x_1^2-(\sqrt{z_1}-\sqrt{z_2})^2}{2\sqrt{z_1z_2}}, \\ |\sqrt{z_1}-\sqrt{z_2}|<\eta x_1, \\ 1>\cos\phi>-1,\quad |\sqrt{z_1}-\sqrt{z_2}|>\eta x_1. \end{cases} \tag{65}$$

Integration of the differential cross section (64) over the region (65) leads to the following contribution:

$$\sigma_{\mathbf{p}_-\|\mathbf{p}_1}=\frac{\alpha^4}{\pi Q_1^2}\mathscr{L}\int_1^{\rho^2}\frac{dz}{z^2}\int_{x_c}^{1-\Delta}dx\int_0^{1-x}dx_2 \times\left[\frac{(1-x)^2+(1-x_1)^2}{(1-x_2)^2}-\frac{4xx_1x_2}{(1-x_2)^2}\right]\left\{\Theta\ln\frac{z}{\eta^2}+\Theta\ln\frac{(x^2\rho^2-z)^2}{x_1^2x^4\rho^4}+\ln\left|\frac{\rho^2(z-x^2)}{z-x^2\rho^2}\right|\right\}. \tag{66}$$

The total contribution of the semicollinear kinematic regions is given by the sum of Eqs. (59), (63), and (66):

$$\sigma_{\text{s-coll}}=\sigma_{\mathbf{p}_+\|\mathbf{p}_-}+\sigma_{\mathbf{p}_+\|\mathbf{q}_1}+\sigma_{\mathbf{p}_-\|\mathbf{p}_1}. \tag{67}$$

5.3. Sum of the contributions of virtual and real pairs

To obtain the final contribution from pair production it is necessary to add to (67) the contribution of the collinear kinematics (53) and the contributions from virtual and soft pairs.

Taking into account the leading and next-to-leading terms, we add the contributions (67) and (53), where the dependence on the parameter η vanishes, and obtain

$$\sigma_{\text{hard}}=\frac{\alpha^4}{\pi Q_1^2}\int_1^{\rho^2}\frac{dz}{z^2}\int_{x_c}^{1-\Delta}dx\left\{\frac{1}{2}L^2R_0(x)+\mathscr{L}[\Theta f(x)+f_1(x)]+\mathscr{L}\int_0^{1-x}dx_2\left[\left(\Theta\ln\frac{(x^2\rho^2-z)^2}{x^2}+\ln\left|\frac{(z-x^2)(\rho^2-z)(z-1)x^2}{z-x^2\rho^2}\right|\right)\varphi-(\Theta\ln(x\rho^2-z)^2+\ln(z-x)^2)\varphi(x,x_2)-(\Theta\ln(x_1^2x^2\rho^4)+\ln x_2^2)\varphi(x_2,x)\right]\right\},\quad L=\ln\frac{Q_1^2z}{m^2},\quad \mathscr{L}=\ln\frac{Q_1^2}{m^2}, \tag{68}$$

where

$$\varphi=\varphi(x,x_2)+\varphi(x_2,x),$$

$$\varphi=(x_2,x)=\frac{(1-x)^2+(x+x_2)^2}{(1-x_2)^2}-\frac{4xx_2(1-x-x_2)}{(1-x_2)^4}.$$

Integrating the third term in curly brackets in (68) over x_2, we obtain the contribution to the cross section for small-angle Bhabha scattering from the emission of real hard pairs:

$$\sigma_{\text{hard}}=\frac{\alpha^4}{\pi Q_1^2}\int_1^{\rho^2}\frac{dz}{z^2}\int_{x_c}^{1-\Delta}dx\left\{\frac{1}{2}L^2(1+\Theta)R_0(x)+\mathscr{L}[\Theta F_1(x)+F_2(x)]\right\},$$

$$F_1(x)=d(x)+C_1(x),\quad F_2(x)=d(x)+C_2(x),$$

$$d(x)=\frac{1}{1-x}\left(\frac{8}{3}\ln(1-x)-\frac{20}{9}\right),$$

$$C_1(x)=-\frac{113}{9}+\frac{142}{9}x-\frac{2}{3}x^2-\frac{4}{3x}-\frac{4}{3}(1+x)\ln(1-x)+\frac{2}{3}\frac{1+x^2}{1-x}\left[\ln\frac{(x^2\rho^2-z)^2}{(x\rho^2-z)^2}-3\text{Li}_2(1-x)\right]+\left(8x^2+3x-9-\frac{8}{x}-\frac{7}{1-x}\right)\ln x+\frac{2(5x^2-6)}{1-x}\ln^2 x+\beta(x)\ln\frac{(x^2p^2-z)^2}{\rho^4},$$

$$C_2(x)=-\frac{122}{9}+\frac{133}{9}x+\frac{4}{3}x^2+\frac{2}{3x}-\frac{4}{3}(1+x)\ln(1-x)+\frac{2}{3}\cdot\frac{1+x^2}{1-x}\left[\ln\left|\frac{(z-x^2)(\rho^2-z)(z-1)}{(x^2\rho^2-z)(z-x)^2}\right|+3\text{Li}_2(1-x)\right]+\frac{1}{3}\left(-8x^2-32x-20+\frac{13}{1-x}+\frac{8}{x}\right)\ln x+3(1+x)\ln^2 x+\beta(x)\ln\left|\frac{(z-x^2)(\rho^2-z)(z-1)}{x^2\rho^2-z}\right|,$$

$$\beta=R_0(x)-\frac{2}{3}\cdot\frac{1+x^2}{1-x}. \qquad (69)$$

Equation (69) describes pair emission from an electron line. To include emission from a positron line in a symmetric experimental setup it is necessary only to multiply this expression by two.

To isolate the dependence on the auxiliary parameter Δ in σ_{hard} we use the relations

$$\int_1^{\rho^2}dz\int_{x_c}^{1-\Delta}dx\Theta(x^2\rho^2-z)=\int_1^{\rho^2}dz\left[\int_{\tilde{x}_c}^{1-\Delta}dx-\int_{\tilde{x}_c}^{1}dx\bar{\Theta}\right],$$

$$\bar{\Theta}=1-\Theta(x^2\rho^2-z),\quad \tilde{x}_c=\max(x_c,\rho^{-1}).$$

Therefore,

$$\int_1^{\rho^2}dz\int_{x_c}^{1-\Delta}\Theta\frac{dx}{1-x}=\int_1^{\rho^2}dz\left[\ln\frac{1-\tilde{x}_c}{\Delta}-\int_{\tilde{x}_c}^{1}\frac{dx}{1-x}\bar{\Theta}\right], \qquad (70)$$

$$\int_1^{\rho^2}dz\int_{x_c}^{1-\Delta}dx\Theta\frac{\ln(1-x)}{1-x}=\int_1^{\rho^2}dz\left[\frac{1}{2}\ln^2(1-\tilde{x}_c)-\frac{1}{2}\ln^2\Delta-\int_{\tilde{x}_c}^{1}dx\frac{\ln(1-x)}{1-x}\bar{\Theta}\right]. \qquad (71)$$

The contribution to small-angle e^+e^- scattering at high energies due to the emission of real soft[13] (with energy less than $\Delta\cdot\varepsilon$) and virtual (29) pairs is given by

$$\sigma_{\text{soft+virt}}=\frac{4\alpha^4}{\pi Q_1^2}\int_1^{\rho^2}\frac{dz}{z^2}\left\{L^2\left(\frac{2}{3}\ln\Delta+\frac{1}{2}\right)+\mathscr{L}\left(-\frac{17}{6}+\frac{4}{3}\ln^2\Delta-\frac{20}{9}\ln\Delta-\frac{4}{3}\zeta_2\right)\right\}.$$

Using Eqs. (70) and (71), it is easy to show that the auxiliary parameter Δ cancels in the sum $\sigma_{\text{pair}}=2\sigma_{\text{hard}}+\sigma_{\text{soft+virt}}$. Now we can write the total contribution of pair production in the final form

$$\sigma_{\text{pair}}=\frac{2\alpha^4}{\pi Q_1^2}\int_1^{\rho^2}\frac{dz}{z^2}\left\{L^2\left(1+\frac{4}{3}\ln(1-x_c)-\frac{2}{3}\int_{x_c}^{1}\frac{dx}{1-x}\bar{\Theta}\right)+\mathscr{L}\left[-\frac{17}{3}-\frac{8}{3}\zeta_2-\frac{40}{9}\ln(1-x_c)+\frac{8}{3}\ln^2(1-x_c)+\int_{x_c}^{1}\frac{dx}{1-x}\bar{\Theta}\left(\frac{20}{9}-\frac{8}{3}\ln(1-x)\right)+\int_{x_c}^{1}dx[L^2(1+\Theta)\bar{R}(x)+\mathscr{L}(\Theta C_1(x)+C_2(x))]\right],$$

$$\bar{R}(x)=\frac{1}{2}R_0(x)-\frac{2}{3(1-x)}. \qquad (72)$$

This expression is the starting point for numerical calculations of the cross section for small-angle Bhabha scattering accompanied by e^+e^- pair production. We note that the leading contribution is described by the electron structure function $D_e^{\bar{e}}(x)$, which gives the probability of finding a positron in an electron with virtual momentum Q^2 with the condition that the electron loses an energy fraction $(1-x)$.[24,27]

In Table I we give the ratio of the cross section σ_{pair} (72) and the normalization cross section σ_0,

$$\sigma_0=\frac{4\pi\alpha^2}{\varepsilon^2\theta_{\min}^2}.$$

TABLE I. The ratio $S=\sigma_{\rm pair}/\sigma_0$ in percent as a function of x_c for NN ($\rho=1.74$, $\theta_{\rm min}=1.61°$) and WW ($\rho=2.10$, $\theta_{\rm min}=1.50°$) detectors; $\sqrt{s}=2\varepsilon=M_Z=91.187$ GeV.

x_c	0.2	0.3	0.4	0.5	0.6	0.7	0.8
S_{NN}, %	−0.018	−0.022	−0.026	−0.029	−0.033	−0.038	−0.046
S_{WW}, %	−0.013	−0.019	−0.024	−0.029	−0.035	−0.042	−0.052

In Table II we illustrate the relation between the nonleading logarithmic contributions containing only the first power of the large logarithm $\mathscr{L}$ and the full expression $\sigma_{\rm pair}$:

$$R=\frac{\sigma_{\rm pair}^{\rm non\text{-}leading}}{\sigma_{\rm pair}}.$$

6. LEADING $\mathscr{O}(\alpha^3)$ CORRECTIONS TO BHABHA SCATTERING

To calculate the leading logarithmic contributions represented by terms of the form $(\alpha\mathscr{L})^3$ we iterate the Lipatov equations[11,13,24] up to β^3 (see Appendix G). We simplified the analytic expressions by using the realistic assumption that the energy threshold for detecting the hard subprocess is small. This allows us to neglect terms of the form

$$x_c^n\left(\frac{\alpha}{\pi}\mathscr{L}\right)^3\sim 10^{-4},\quad n=1,\ 2,\ 3.$$

This implies that we can limit ourselves to only inclusion of the radiation of the initial electron and positron.

The contribution to Σ due to the emission of three either real or virtual photons is written as

$$\Sigma^{3\gamma}=\frac{1}{4}\left(\frac{\alpha}{\pi}\mathscr{L}\right)^3\int_1^{\rho^2}dz\,z^{-2}\int_{x_c}^1 dx_1\int_{x_c}^1 dx_2\Theta(x_1x_2-x_c)$$
$$\times\left[\frac{1}{6}\delta(1-x_2)P^{(3)}(x_1)\Theta(x_1^2\rho^2-z)\right.$$
$$\left.+\frac{1}{2x_1^2}P^{(2)}(x_1)P(x_2)\Theta_1\Theta_2\right],$$

where $P(x)$ and $P^{(2)}(x)$ are given by (24) and (50),

$$\Theta_1\Theta_2=\Theta\left(z-\frac{x_2^2}{x_1^2}\right)\Theta\left(\rho^2\frac{x_2^2}{x_1^2}-z\right),$$

$$P^{(3)}(x)=\delta(1-x)\Delta_t+\Theta(1-x-\Delta)\theta_t,$$

$$\Delta_t=48\left[\frac{1}{3}\zeta_3-\frac{1}{2}\zeta_2\left(\ln\Delta+\frac{3}{4}\right)+\frac{1}{6}\left(\ln\Delta+\frac{3}{4}\right)^3\right],$$

$$\theta_t=48\left\{\frac{1}{2}\frac{1+x^2}{1-x}\left[\frac{9}{32}-\frac{1}{2}\zeta_2+\frac{3}{4}\ln(1-x)-\frac{3}{8}\ln x\right.\right.$$
$$\left.+\frac{1}{2}\ln^2(1-x)+\frac{1}{12}\ln^2 x-\frac{1}{2}\ln x\ln(1-x)\right]$$
$$+\frac{1}{8}(1+x)\ln x\ln(1-x)-\frac{1}{4}(1-x)\ln(1-x)$$
$$+\frac{1}{32}(5-3x)\ln x-\frac{1}{16}(1-x)-\frac{1}{32}(1+x)\ln^2 x$$
$$\left.+\frac{1}{8}(1+x)\mathrm{Li}_2(1-x)\right\}.\qquad(73)$$

Let us now consider the contribution to Σ from the process with e^+e^- pair production and simultaneous photon emission. Both the pair and the photon can be either real or virtual. We shall take into account the singlet and nonsinglet pair production mechanisms (only the singlet mechanism was considered in Ref. 24). The result is

$$\Sigma^{e^+e^-\gamma}=\frac{1}{4}\left(\frac{\alpha}{\pi}\mathscr{L}\right)^3\int_1^{\rho^2}\frac{dz}{z^2}\int_{x_c}^1 dx_1\int_{x_c}^1 dx_2\Theta(x_1x_2$$
$$-x_c)\left\{\frac{1}{3}\left[R^P(x_1)+\frac{1}{3}P^{(2)}(x_1)\right.\right.$$
$$\left.+\frac{2}{3}R(x_1)\right]\delta(1-x_2)\Theta(x_1^2\rho^2-z)$$
$$\left.+\frac{1}{2x_1^2}P(x_2)R(x_1)\Theta_1\Theta_2\right\}(1+\mathscr{O}(x_c^3)),$$

where

$$R(x)=R^s(x)+\frac{2}{3}P(x),$$

$$R^s(x)=\frac{1-x}{3x}(4+7x+4x^2)+2(1+x)\ln x,$$

TABLE II. Values of the relative contribution of nonleading terms to pair production, R, for NN and WW detectors (see caption to Table I).

x_c	0.2	0.3	0.4	0.5	0.6	0.7	0.8
R_{NN}	0.036	−0.122	−0.194	−0.238	−0.268	−0.335	−0.465
R_{WW}	0.179	−0.021	−0.088	−0.120	−0.179	−0.271	−0.415

$$R^P(x)=R^s(x)\left(\frac{3}{2}+2\ln(1-x)\right)+(1+x)(-\ln^2 x+4\mathrm{Li}_2(1-x))+\frac{1}{3}(-9-3x+8x^2)\ln x+\frac{2}{3}\left(-\frac{3}{x}-8+8x+3x^2\right)+\frac{2}{3}P^{(2)}(x).$$

7. THE CALORIMETRIC EXPERIMENTAL SETUP

In the calorimetric experimental setup, events in which an electron (positron) is incident on a small area of the detector simultaneously with one or more photons, so that a single cluster is seen, are indistinguishable from events in which a single electron (positron) hits the same area of the detector if the energy release is the same. This situation is described by introducing a small angle δ determined by the detector parameters, so that when the relative angle between the electron and the accompanying photon is smaller than δ these particles are detected as a single one. We note that here, as above, we are assuming that charged and uncharged particles are distinguished in the detection process. For the detectors of LEP I the parameter δ is of order 10×10^{-3} rad, which is comparable to the angular span of the detectors and the minimum scattering angle. An example of realistic conditions is

$$\theta_1=\theta_{\min}=24\times 10^{-3}\ \text{rad},\quad \theta_{\max}=\rho\theta_1=58\times 10^{-3}\ \text{rad}. \tag{74}$$

Therefore, edge effects can be important, and the expressions for the contributions to Σ become more complicated. In this case it is naturally advantageous to use the Monte Carlo method. Nevertheless, fairly accurate results can also be obtained analytically. First, in the orders $(L\alpha/\pi)^2$ and $(L\alpha/\pi)^3$ it is necessary to discard the contributions corresponding to emission along the scattered electron and positron, i.e., to keep only terms containing $\Theta(x^2\rho^2-z)$ in (49) and (72).

It is convenient to write the contribution of corrections of order α/π from the emission of a single hard photon [see (19)] as

$$\Sigma^{\gamma}=\frac{\alpha}{\pi}(\Sigma_i^{\gamma}+\Sigma_f^{\gamma}), \tag{75}$$

where the term Σ_i^{γ} describing the contribution from emission by the initial electron has the same form as before:

$$\Sigma_i^{\gamma}=\int_1^{\rho^2}\frac{dz}{z^2}\left\{2(1-L)\ln\frac{1}{\Delta}+\frac{3}{2}L-2+\int_{x_c}^{1-\Delta}dx\,\frac{1+x^2}{1-x}\left[\left(L-1+L_2+\frac{(1-x)^2}{1+x^2}\right)\Theta(x^2\rho^2-z)+L_3\Theta(z-x^2\rho^2)\right]\right\}. \tag{76}$$

For the second term we find

$$\Sigma_f^{\gamma}=\int_1^{\rho^2}\frac{dz}{z^2}\left\{\int_0^1 dx\,\frac{1+x^2}{1-x}\ln\left|\frac{(d_--z)(d_+-z)x^2}{(xd_--z)(xd_+-z)}\right|+\int_{x_c}^1 dx\,\frac{1+x^2}{1-x}\left[\ln\left|\frac{(\rho^2-z)(z-1)}{(z-x)(\rho^2x-z)}\right|+\ln\left|\frac{(xd_+-z)(xd_--z)}{(d_+-z)(d_--z)}\right|\right]\right\},$$

$$d_{\pm}=\left(\sqrt{z}\pm(1-x)\frac{\delta}{\theta_1}\right)^2. \tag{77}$$

This result (like that in Sec. 3) is derived by integrating the term proportional to $1/\sqrt{a_2}$ in (19), where it is convenient to split the integral over the rectangle $1<z<\rho^2$, $x^2<z_1<x^2\rho^2$ into the following five regions:

1) $x^2<z_1<x^2z-\eta$, 2) $x^2z-\eta<z_1<x^2z-\eta_1$,

3) $x^2z-\eta_1<z_1<x^2z+\eta_1$,

4) $x^2z+\eta_1<z_1<x^2z+\eta$,

5) $xz^2+\eta<z_1<x^2\rho^2$, $\eta=2x^2(1-x)\sqrt{z}\,\frac{\delta}{\theta_1}$.

The dependence on the auxiliary parameter η_1 vanishes in the complete sum of contributions from the different regions.

8. ESTIMATE OF THE DISCARDED TERMS AND THE ACCURACY OF THE CALCULATIONS

Let us now discuss the terms not involved in the calculation, owing to the required accuracy (1). They fall into several groups.

(a) The higher-order electroweak contributions do not exceed

$$\Sigma_{EW}^{\text{h.o.}}=\frac{\alpha Q_1^2}{\pi M_Z^2}\leqslant 10^{-4}. \tag{78}$$

(b) In calculating the bremsstrahlung contribution in lowest-order perturbation theory we have considered only graphs of the scatterer type and have neglected the contributions of graphs of the annihilation type. We have thus neglected contributions from virtual and real radiative corrections of the form

$$\theta_1^2\frac{\alpha}{\pi}\ln^2\frac{s}{-t}\leqslant 10^{-4}. \tag{79}$$

We note that our result for Σ^{γ} is numerically consistent with the results obtained by other authors,[1] who used the exact matrix element.[25]

(c) In the bremsstrahlung calculation we have also neglected the interference contributions of the scatterer and annihilation graphs:

$$\theta_1^2\frac{\alpha}{\pi}L\leqslant 10^{-4} \tag{80}$$

and the corresponding terms in double bremsstrahlung:

$$\theta_1^2\left(\frac{\alpha L}{\pi}\right)^2\leqslant 10^{-4}. \tag{81}$$

TABLE III. Values of δ_i for the NN detector for $\theta_{\min}^{NN}=26.125$ mrad, $\theta_{\max}^{NN}=55.875$ mrad, $\sqrt{s}=92.3$ GeV.

	NN-detector, $\rho=1.97$								
x_c	0.1	0.2	0.3	0.4	0.5	0.6	0.7	0.8	0.9
δ_0	4.13	4.13	4.13	4.13	4.13	4.13	4.13	4.13	4.13
δ^{γ}	−6.84	−7.17	−7.44	−8.16	−8.94	−10.32	−12.67	−16.73	−24.98
$\delta^{\gamma\gamma}_{\text{lead}}$	0.01	0.00	−0.01	−0.02	−0.05	−0.08	−0.05	0.13	0.87
$\delta^{\gamma}_{\gamma\text{lead}}$	0.49	0.46	0.42	0.36	0.27	0.17	0.14	0.25	0.93
$\delta^{\gamma\gamma}_{n\text{-lead}}$	0.07	0.08	0.08	0.08	0.09	0.09	0.09	0.06	−0.03
$\delta^{\gamma}_{\gamma n\text{-lead}}$	0.06	0.05	0.04	0.04	0.04	0.05	0.05	0.03	−0.02
$\delta^{e^+e^-}$	−0.00	−0.02	−0.02	−0.03	−0.04	−0.05	−0.06	−0.07	−0.09
$\delta^{e^+e^-\gamma}$	0.008	0.006	0.005	0.004	0.004	0.003	0.003	0.003	0.006
$\delta^{3\gamma}$	−0.05	−0.04	−0.04	−0.04	−0.03	−0.03	−0.02	−0.01	−0.01
$\Sigma\delta_i$	−2.11	−2.50	−2.82	−3.60	−4.51	−6.99	−8.37	−12.19	−19.19

(d) We have neglected interference contributions to pair production of the up–down type (on the electron and on the positron), including those from taking into account the identical nature of the fermions:

$$\theta_1^2\left(\frac{\alpha}{\pi}\right)^2 L^3\leqslant 10^{-4}. \tag{82}$$

(e) The eikonal form of the amplitude taking into account multiphoton exchanges in the scattering channel is violated by terms of the form

$$\theta_1^2\,\frac{\alpha}{\pi}\leqslant 10^{-4}. \tag{83}$$

(f) Pair production of heavy fermions (μ, τ; virtual and real) and also the production of real pairs of pions introduces a contribution at least an order of magnitude smaller than that of light fermions.[9]

(g) The contributions of higher orders of perturbation theory in the leading approximation are of order

$$\left(\frac{\alpha L}{\pi}\right)^n\leqslant 10^{-4},\quad n\geqslant 4.$$

Treating these as independent estimates and combining them, we can state that the physical uncertainty in our expressions satisfies the requirement (1):

$$\left|\frac{\delta\sigma_{\text{phys}}}{\sigma}\right|<10^{-3}.$$

9. NUMERICAL RESULTS AND THEIR DISCUSSION

We have presented the cross section for small-angle Bhabha scattering in two forms of equivalent accuracy:

$$\sigma=\frac{4\pi\alpha^2}{Q_1^2}\{\Sigma_0+\Sigma^{\gamma}+\Sigma^{2\gamma}+\Sigma^{e^+e^-}+\Sigma^{3\gamma}+\Sigma^{e^+e^-\gamma}\},$$

$$\sigma=\frac{4\pi\alpha^2}{Q_1^2}\Sigma_{00}\{1+\delta_0+\delta^{\gamma}+\delta^{2\gamma}+\delta^{e^+e^-}+\delta^{3\gamma}+\delta^{e^+e^-\gamma}\},$$

where

$$\Sigma_{00}=\Sigma_0|_{\Pi=0}=1-\rho^{-2}+\Sigma_W+\Sigma_\theta,$$

$$\delta_0=\frac{\Sigma_0-\Sigma_{00}}{\Sigma_{00}},\quad \delta^{\gamma}=\frac{\Sigma^{\gamma}}{\Sigma_{00}},\dots .$$

The Born cross section

$$\sigma^B=\frac{4\pi\alpha^2}{Q_1^2}\Sigma_0$$

for $\theta_1=26.125$ mrad and $\theta_2=55.875$ mrad, corresponding to the NN detector, is $\sigma^B=148.186$ nb at $\sqrt{s}=92.3$ GeV, and for $\theta_1=24$ mrad and $\theta_2=58$ mrad (the WW detector) it is $\sigma^B=175.588$ nb at the same energy. The results of our calculations are presented in Tables III and IV and in Fig. 4.

TABLE IV. Values of δ_i for the WW detector for $\theta_{\min}^{WW}=24$ mrad, $\theta_{\max}^{WW}=58$ mrad, $\sqrt{s}=92.3$ GeV.

	WW-detector, $\rho=2.42$								
x_c	0.1	0.2	0.3	0.4	0.5	0.6	0.7	0.8	0.9
δ_0	4.05	4.05	4.05	4.05	4.05	4.05	4.05	4.05	4.05
δ^{γ}	−5.87	−6.22	−6.66	−7.24	−8.14	−9.69	−12.18	−16.35	−24.65
$\delta^{\gamma\gamma}_{\text{lead}}$	−0.01	−0.02	−0.04	−0.06	−0.10	−0.12	−0.09	0.09	0.84
$\delta^{\gamma}_{\gamma\text{lead}}$	0.45	0.41	0.36	0.29	0.18	0.10	0.07	0.20	0.89
$\delta^{\gamma\gamma}_{n\text{-lead}}$	0.07	0.07	0.08	0.08	0.09	0.09	0.08	0.06	−0.03
$\delta^{\gamma}_{\gamma n\text{-lead}}$	0.05	0.04	0.04	0.04	0.05	0.05	0.05	0.03	−0.05
$\delta^{e^+e^-}$	0.00	−0.01	−0.02	−0.03	−0.03	−0.04	−0.05	−0.07	−0.08
$\delta^{e^+e^-\gamma}$	−0.012	−0.007	−0.004	−0.002	−0.001	−0.001	0.000	0.001	0.004
$\delta^{3\gamma}$	−0.026	−0.024	−0.021	−0.018	−0.013	−0.007	0.000	0.009	0.015
$\Sigma\delta_i$	−1.32	−1.72	−2.23	−2.89	−3.93	−5.56	−8.06	−11.97	−19.02

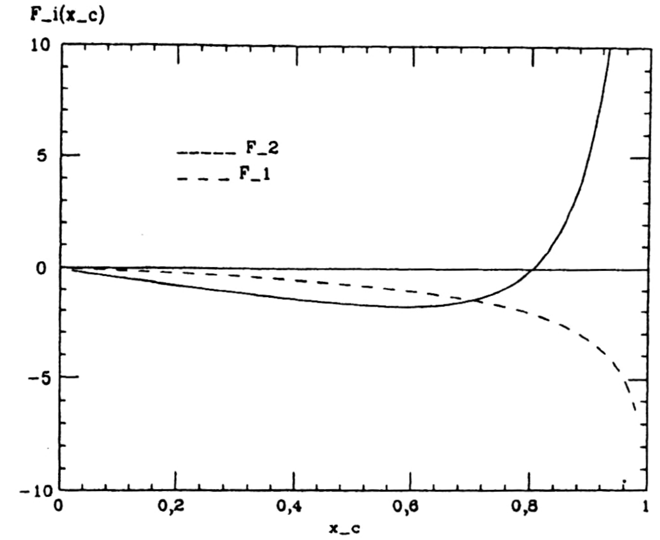

FIG. 3. Values of the integrals of the kernels of the evolution equations $F_i=\int_{x_c}^1 P^{(i)}(x)dx$ as functions of the lower limit.

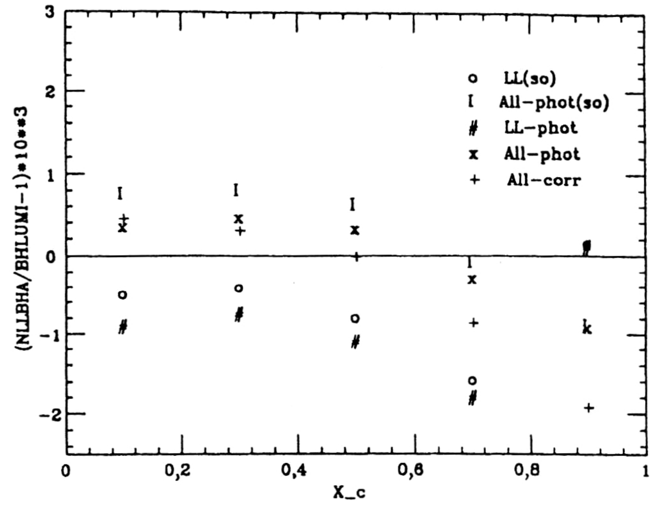

FIG. 4. Value of $(\sigma_{\rm NLLBHA}/\sigma_{\rm BHLUMI}-1)$ in percent as a function of x_c, taking into account the various contributions. The $\sigma_{\rm NLLBHA}$ are the results of the approach described here, and the $\sigma_{\rm BHLUMI}$ are the results of the Jadach group.

Let us discuss some of the main features of the radiative corrections. The sign of each of the contributions Σ_i can change, depending on the ratio of the virtual and real contributions. The cross section corresponding to the contributions of graphs in the Born approximation is positive, while the sign of the radiative corrections depends on the order of perturbation theory: it is negative for contributions of odd order and positive for ones of even order. When the aperture of the counters is large and the energy threshold for detection is small, there is complete cancellation of the leading-log contributions, owing to the Kinoshita–Lee–Nauenberg theorem. As the aperture decreases and the parameter x_c increases the cancellation of the virtual and real contributions to the radiative corrections becomes incomplete. Consequently, the radiative corrections for the *NN* case are larger in absolute value than those for the *WW* case. We also see from Tables III and IV that as the detection threshold x_c increases, the contributions from the emission of real particles are suppressed, and the radiative corrections, which become negative, grow in magnitude.

We note that the ratio of the leading and nonleading contributions to $\Sigma^{2\gamma}$ is not always much larger than unity (in modulus). As can be seen from the graph of Fig. 3, which represents the behavior of the function $F_2(x)=\int_x^1 P^{(2)}\times(y)dy$ describing the typical contribution in the leading-log approximation, this function passes through zero at $x\approx 0.8$. This shows that significant internal cancellations can occur in the leading contributions; this, of course, depends strongly on the choice of the parameter x_c and the angular range.

In Fig. 4 we compare our results obtained using the NLLBHA program with the results of the Jadach group obtained using the BHLUMI program and the Monte Carlo method. We have chosen the parameter values for the *WW* detector (see Table IV). We see that the results agree at the 0.1% level for a wide range of values of the parameter x_c when photon emission is included. We also see from Fig. 4 that for $x_c\sim 0.8$ the contribution of nonleading terms is important. The pair contribution (which is neglected in the BHLUMI program) is less than 0.1% everywhere except for $x_c\gtrsim 0.8$, where it must be included.

ACKNOWLEDGMENTS

The authors would like to thank V. S. Fadin, L. N. Lipatov, N. P. Merenkov, and L. Trentadue for coauthoring the studies on which this review is based. The authors would also like to thank D. Bardin, F. Berends, B. Ward, E. Levin, B. Pieterzyk, M. Skrzypek, J. Field, and S. Jadach for very useful discussions during the various stages of this study. É. A. Kuraev thanks the INTAS fund (grant 93-1867) for partial support. A. B. Arbuzov thanks the Swedish Royal Academy of Sciences for financial support in the form of an ICFPM grant.

APPENDIX A: KINEMATICS OF THE INFINITE-MOMENTUM FRAME. SINGLE BREMSSTRAHLUNG

For the process

$$e^+(p_2)+e^-(p_1)\to e^+(q_2)+e^-(q_1)+\gamma(k)$$

it is convenient to introduce the Sudakov parametrization for the 4-momenta of the final particles:

$$q_1=\alpha_1\tilde{p}_2+\beta_1\tilde{p}_1+\mathbf{q}_1^\perp, \quad q_2=\alpha_2\tilde{p}_2+\beta_2\tilde{p}_1+\mathbf{q}_2^\perp,$$
$$k=\alpha\tilde{p}_2+\beta\tilde{p}_1+\mathbf{k}^\perp, \tag{84}$$

where $\tilde{p}_{1,2}$ are 4-vectors lying nearly on the light cone, and $\mathbf{q}_i^\perp$ and $\mathbf{k}^\perp$ are Euclidean 2-vectors given in the c.m. frame:

$$\mathbf{q}_i^\perp\mathbf{p}_2=\mathbf{q}_i^\perp\mathbf{p}_1=0, \quad (\mathbf{q}_i^\perp)^2=-\mathbf{q}_i^2<0, \quad i=1,2;$$

$$\tilde{p}_1=p_1-\frac{m^2}{s}p_2, \quad \tilde{p}_2=p_2-\frac{m^2}{s}p_1,$$

$$p_1^2=p_2^2=q_1^2=q_2^2=m^2, \quad k^2=0, \quad \tilde{p}_1^2=\tilde{p}_2^2=\frac{m^6}{s^2},$$

$$s=2p_1p_2=2\widetilde{p}_1\widetilde{p}_2=2\widetilde{p}_1p_2=2\widetilde{p}_2p_1\gg m^2.$$

We shall consider the kinematic situation in which the photon is emitted at a small angle relative to the direction of motion of the initial electron. The mass-shell conditions for the 4-momenta lead to the identities

$$q_1^2=s\alpha_1\beta_1-(\mathbf{q}_1^\perp)^2=m^2,\quad \alpha_1=\frac{(\mathbf{q}_1^\perp)^2+m^2}{s\beta_1},$$

$$q_2^2=s\alpha_2\beta_2-(\mathbf{q}_2^\perp)^2=m^2,\quad \beta_2=\frac{(\mathbf{q}_2^\perp)^2+m^2}{s\alpha_2},$$

$$k^2=s\alpha\beta-(\mathbf{k}^\perp)^2=0,\quad s\alpha=\frac{(\mathbf{k}^\perp)^2}{\beta},$$

$$\alpha_2=1,\quad |\beta_2|\sim|\alpha_1|\sim|\alpha|\ll 1,\quad \beta_1\sim\beta\sim 1.$$

Using the expression $d^4q_1=(s/2)d\alpha_1 d\beta_1 d^2\mathbf{q}_1^\perp$, we can represent the phase space as

$$d\phi=\frac{d^3\mathbf{q}_1d^3\mathbf{q}_2d^3\mathbf{k}}{2q_1^02q_2^02k^0}\delta^{(4)}(p_1+p_2-q_1-q_2-k)$$

$$=\frac{1}{4s\beta\beta_1}d\beta d\beta_1\delta(1-\beta-\beta_1)d^2\mathbf{k}^\perp d^2\mathbf{q}_1^\perp d^2\mathbf{q}_2^\perp \times\delta^{(2)}(\mathbf{q}_1^\perp+\mathbf{q}_2^\perp+\mathbf{k}^\perp).$$

The energy–momentum conservation law can be written as

$$q+p_1=q_1+k,\quad p_2=q_2+q,\quad \mathbf{q}^\perp=-\mathbf{q}_2^\perp.$$

Let us give the expressions for the denominators of the propagators (here $\beta_1=x$ and $\beta=1-x$):

$$(p_1-k)^2-m^2=\frac{-d_1}{1-x},\quad (p_1+q)^2-m^2=\frac{d}{x(1-x)},$$

$$q^2=-(\mathbf{q}_2^\perp)^2,\quad d=m^2(1-x)^2+(\mathbf{q}_1^\perp-\mathbf{q}_2^\perp x)^2,$$

$$d_1=m^2(1-x)^2+(\mathbf{q}_1^\perp-\mathbf{q}_2^{\perp 1})^2. \qquad (85)$$

The matrix element of the process takes the form

$$M=\frac{g^{\mu\nu}}{q^2}\bar{v}(p_2)\gamma_\mu v(q_2)\bar{u}(q_1)O_\nu u(p_1),$$

$$O^\nu=\gamma^\nu\frac{\hat{p}_1-\hat{k}+m}{(p_1-k)^2-m^2}\hat{e}+\hat{e}\frac{\hat{p}_1+\hat{q}+m}{(p_1+q)^2-m^2}\gamma^\nu.$$

It is helpful to use the following decomposition of the tensor $g_{\mu\nu}$:

$$g_{\mu\nu}=g_{\mu\nu}^\perp+\frac{p_1^\mu p_2^\nu+p_1^\nu p_2^\mu}{p_1p_2}\simeq\frac{2p_1^\mu p_2^\nu}{s}\left(1+\mathcal{O}\left(\frac{(\mathbf{q})^2}{s}\right)\right).$$

Using (84) and (85), we can write

$$p_2^\nu\bar{u}(q_1)O_\nu u(p_1)\equiv\bar{u}(q_1)\hat{v}_\rho u(p_1)e_\rho(k),$$

where the generalized vertex v_ρ is written as

$$v_\rho=s\gamma_\rho x(1-x)\left(\frac{1}{d}-\frac{1}{d_1}\right)-\frac{\gamma_\rho\hat{k}\hat{p}_2}{d}x(1-x)-\frac{\hat{p}_2\hat{k}\gamma_\rho}{d_1}(1-x).$$

Let us transform the sum over spin states of the squared matrix element:

$$\sum_{\text{spin}}|\bar{v}(q_2)\hat{p}_1v(p_2)|^2=\text{Tr}\,\hat{p}_2\hat{p}_1\hat{p}_2\hat{p}_1=2s^2,$$

$$R=\frac{-1}{4s^2}\text{Tr}(\hat{p}_1+m)\hat{v}_\mu(\hat{p}_1+\hat{k}-\hat{q}+m)\hat{v}_\mu$$

$$=x[-2xm^2(d-d_1)^2+(\mathbf{q}_2^\perp)^2(1+x^2)dd_1]\frac{1}{d^2d_1^2}.$$

In the end we obtain

$$d\sigma^{e^+e^-\to e^+(e^-\gamma)}=2\alpha^3\frac{d^2\mathbf{q}_1^\perp d^2\mathbf{q}_2^\perp dx(1-x)}{\pi^2(\mathbf{q}_2^\perp)^4(dd_1)^2}[-2xm^2(d-d_1)^2+(\mathbf{q}_2^\perp)^2(1+x^2)dd_1].$$

We thus obtain the differential cross section for double bremsstrahlung in different directions:

$$\frac{d\sigma^{e^+e^-\to e^+\gamma e^-\gamma}}{d^2\mathbf{q}_1^\perp d^2\mathbf{q}_2^\perp dx_1dx_2}=\frac{\alpha^4(1+x_1^2)(1+x_2^2)}{\pi^4(1-x_1)(1-x_2)}\times\int\frac{d^2\mathbf{q}^\perp}{(\mathbf{q}^\perp)^4}\left[\frac{(\mathbf{q}^\perp)^2(1-x_1)^2}{d_1d_2}-\frac{2x_1}{1+x_1^2}\frac{m^2(1-x_1)^2(d_1-d_2)^2}{d_1^2d_2^2}\right]\times\left[\frac{(\mathbf{q}^\perp)^2(1-x_2)^2}{\widetilde{d}_1\widetilde{d}_2}-\frac{2x_2}{1+x_2^2}\frac{m^2(1-x_2)^2(\widetilde{d}_2-\widetilde{d}_1)^2}{\widetilde{d}_1^2\widetilde{d}_2^2}\right],$$

where x_1, $\mathbf{q}_1^\perp$ and x_2, $\mathbf{q}_2^\perp$ are the energy fractions and momentum components transverse to the initial beam direction of the scattered electron and positron, respectively, $\mathbf{q}^\perp$ are the transverse components of the virtual-photon momentum, and

$$d_1=(1-x_1)^2m^2+(\mathbf{q}_1^\perp-\mathbf{q}^\perp x_1)^2,$$

$$d_2=(1-x_1)^2m^2+(\mathbf{q}_1^\perp-\mathbf{q}^\perp)^2,$$

$$\widetilde{d}_1=(1-x_2)^2m^2+(\mathbf{q}_2^\perp+\mathbf{q}^\perp x_2)^2,$$

$$\widetilde{d}_2=(1-x_2)^2m^2+(\mathbf{q}_2^\perp+\mathbf{q}^\perp)^2.$$

Let us now consider the experimental limits (4) on the range of integration over $d^2\mathbf{q}_1^\perp$ and $d^2\mathbf{q}_2^\perp$. We define the dimensionless variables

$$z_{1,2}=\frac{(\mathbf{q}_{1,2}^\perp)^2}{Q_1^2}.$$

The two narrow bands $z_1 \simeq z_2$ and $z_1 \simeq x^2 z_2$ in the region of integration in the (z_1, z_2) plane give logarithmically enhanced contributions. Therefore, the leading-log contribution to Σ^H will be selected when at least one of these bands intersects the rectangle $x^2 < z_1 < \rho^2 x^2$, $1 < z_2 < \rho^2$. We note that the band $z_1 \simeq x^2 z_2$ corresponding to the emission of a single hard photon along the direction of motion of the scattered electron is the diagonal of this rectangle. The band $z_1 \simeq z_2$ corresponding to the emission of a hard photon along the direction of motion of the initial electron intersects the rectangle if $x^2\rho^2 > z_2$ and $x\rho > 1$. These conditions give the Θ functions in the leading contribution to Σ^H.

Actually, for the contribution from radiation by the initial electron [see (19)] we obtain

$$F_1 = \Theta(1-\rho x) \int_1^{\rho^2} \frac{dz_2}{z_2^2} \int_{x^2}^{x^2\rho^2} \frac{dz_1 z_2 (1-x)}{(z_1 - x z_2)(z_2 - z_1)} + \Theta(x\rho - 1) \int_{x^2\rho^2}^{\rho^2} \frac{dz_2}{z_2^2} \int_{x^2}^{x^2\rho^2} \frac{dz_1 z_2 (1-x)}{(z_1 - x z_2)(z_2 - z_1)} + \Theta(x\rho - 1) \int_1^{x^2\rho^2} \frac{dz_2}{z_2^2} \left\{ \int_{x^2}^{z_2 - \eta} \frac{dz_1 (1-x) z_2}{(z_1 - x z_2)(z_2 - z_1)} + \int_{z_2+\eta}^{x^2\rho^2} \frac{dz_1 (1-x) z_2}{(z_1 - x z_2)(z_1 - z_2)} + \int_{z_2-\eta}^{z_2+\eta} \frac{dz_1}{[(z_2 - z_1)^2 + 4\sigma^2 z_2]^{1/2}} - \frac{2x\sigma^2}{1+x^2} \int_{z_2-\eta}^{z_2+\eta} \frac{2 dz_1 z_2}{[(z_2-z_1)^2 + 4\sigma^2 z_2]^{3/2}} \right\},$$

where we have introduced the auxiliary parameter η:

$$\sigma^2 \ll \eta \ll 1.$$

We see that by this trick the result can be obtained in analytic form, where the η dependence vanishes in the sum:

$$F_1 = \int_1^{\rho^2} \frac{dz}{z^2} \left\{ \Theta(x\rho - 1)\Theta(x^2\rho^2 - z) \left(L - \frac{2x}{1+x^2} \right) + \Theta(x\rho - 1)\Theta(z - x^2\rho^2) L_2 + (\Theta(1 - x\rho) + \Theta(x\rho - 1)\Theta(z - x^2\rho^2)) L_3 \right\}.$$

Similarly, we obtain the contribution from emission along the scattered electron:

$$F_2 = \int_1^{\rho^2} \frac{dz}{z^2} \left\{ L - \frac{2x}{1+x^2} + L_1 \right\},$$

where $L = \ln(Q_1^2 z/m^2)$, and L_1, L_2, and L_3 are given in (22).

APPENDIX B: VIRTUAL CORRECTIONS TO ONE-PHOTON EMISSION

The differential cross section for high-energy electron–positron scattering acompanied by the emission of a single hard photon can be written as

$$d\sigma^{H(S+V)} = \frac{\alpha^3 dx d^2 q_2 d^2 q_1}{2\pi^2 x(1-x)((\mathbf{q}_2^\perp)^2)^2} R,$$

$$R = \lim_{(p_1 p_2)\to\infty} \frac{4 p_{2\rho} p_{2\sigma} k_{\rho\sigma}}{(2 p_1 p_2)^2}.$$

The tensor $k_{\rho\sigma}$ entering into R is related to the matrix element $\varepsilon_\rho M_\rho$ of Compton scattering (where ε_ρ is the polarization vector of a *heavy* photon) as

$$k_{\rho\sigma} = \sum_{\text{spin}} M_\rho M_\sigma^* = \tilde{g}_{\rho\sigma} k_g + \tilde{p}_{1\rho}\tilde{p}_{1\sigma} k_{11} + \tilde{q}_{1\rho}\tilde{q}_{1\sigma} k_{22} + \tilde{q}_{1\rho}\tilde{p}_{1\sigma} k_{21} + \tilde{p}_{1\rho}\tilde{q}_{1\sigma} k_{12},$$

$$k_{ij} = B_{ij} + \frac{\alpha}{2\pi} T_{ij}, \quad i,j = 1,2, \quad k_g = B_g + \frac{\alpha}{2\pi} T_g,$$

where

$$\tilde{g}_{\rho\sigma} = g_{\rho\sigma} - \frac{q_\rho q_\sigma}{q^2}, \quad \tilde{p}_{1\rho} = p_{1\rho} - \frac{p_1 q}{q^2} q_\rho,$$

$$\tilde{q}_{1\rho} = q_{1\rho} - \frac{q_1 q}{q^2} q_\rho,$$

which are explicitly gauge-invariant combinations of momenta: $k_{\rho\sigma} q_\rho = k_{\rho\sigma} q_\sigma = 0$.

In the case of small-angle scattering of interest here, R is written as

$$R = \left(1 + \frac{\alpha}{2\pi} \eta \right) (B_{11}(s_1, t_1) + x^2 B_{11}(t_1, s_1)) + \frac{\alpha}{2\pi} T,$$

$$T = T_{11} + x^2 T_{22} + x(T_{12} + T_{21}),$$

where η is given in (39).

Exact expressions for T_{ik} are given in Ref. 20. We need these only in the limiting case where $s_1 \ll |t_1|$ and $|t_1| \ll s_1$, for fixed q^2 and $u_1 = -2 p_1 q_1$.

In the case of small s_1 we have

$$s = \frac{1}{x(1-x)} [m^2(1-x)^2 + (\mathbf{q}_2^\perp x + \mathbf{q}_1^\perp)^2].$$

In the rest of this appendix we shall omit the subscript 1 for the invariants s and t characterizing the Compton subprocess; see (41).

Using the fact that at small s we will have $q^2 = -(\mathbf{q}_2^\perp)^2$, $t = -(1-x)(\mathbf{q}_2^\perp)^2$, and $u = -(\mathbf{q}_2^\perp)^2 x$, we obtain the following expressions for T and η:

$$\eta_{s \ll |t|} = 2(L - 1 + \ln x)(2 \ln \Delta - \ln x) + 3L - \ln^2 x - \frac{9}{2},$$

$$T_{s\ll|t|} = \frac{2}{s(1-x)} \left\{ 4(1+x^2) \left[\ln x \ln \frac{(\mathbf{q}_2^\perp)^2}{s} - \mathrm{Li}_2(1-x) \right] - 1 + 2x + x^2 \right\} - \frac{16 m^2}{s^2} l_q \ln x.$$

For small $|t|$ we have

$$\eta_{|t| \ll s} = 2(L - 1 - \ln x)(2 \ln \Delta - \ln x) + 3L - \ln^2 x - \frac{9}{2},$$

$$T_{|t|\ll s}=\frac{2x}{t(1-x)}\left\{4(1+x^2)\left[\ln x\ln\frac{(\mathbf{q}_2^\perp)^2}{-t}-\frac{1}{2}\ln^2 x-\mathrm{Li}_2(1-x)\right]-1-2x+x^2\right\}+\frac{16m^2x^2}{t^2}l_q\ln x.$$

The rest of the integration is trivial. We shall give only the most important steps. The contribution of the terms containing η can be represented in a form analogous to that of the Born contribution:

$$\Sigma_\eta^{H(S+V)}=\frac{1}{2}\left(\frac{\alpha}{\pi}\right)^2\int_1^{\rho^2}\frac{dz}{z^2}L\int_{x_c}^{1-\Delta}dx\,\frac{1+x^2}{1-x}\left\{(1+\Theta(\rho^2x^2-z))\left[L\left(2\ln\Delta-\ln x+\frac{3}{2}\right)+(2\ln\Delta-\ln x)(\ln x-2)-\frac{1}{2}\ln^2 x-\frac{15}{4}\right]+\left(2\ln\Delta-\ln x+\frac{3}{2}\right)k(x,z)-2\ln x(2\ln\Delta-\ln x)\Theta(\rho^2x^2-z)\right\}.$$

To obtain the contribution of terms containing T it is necessary to first study the following types of integral:

$$I_{s\{t\}}=Q_1^2\int\frac{d^2\mathbf{q}_2^\perp}{\pi(\mathbf{q}_2^\perp)^4}\int\frac{d^2\mathbf{q}_1^\perp}{\pi s\{t\}}\ln\frac{(\mathbf{q}_2^\perp)^2}{s\{-t\}},$$

$$i_{s\{t\}}=Q_1^2\int\frac{d^2\mathbf{q}_2^\perp}{\pi(\mathbf{q}_2^\perp)^4}\int\frac{d^2\mathbf{q}_2^\perp}{\pi s\{t\}},$$

$$m_{s\{t\}}=Q_1^2\int\frac{d^2\mathbf{q}_2^\perp}{\pi(\mathbf{q}_2^\perp)^4}\int\frac{d^2\mathbf{q}_1^\perp m^2}{\pi s^2\{t^2\}}.$$

Writing $\sigma^2(1-x)^2+(\mathbf{q}_2^\perp x-\mathbf{q}_1^\perp)^2/Q_1^2$ as $a+b\cos\phi$ and using the integrals

$$\int_0^{2\pi}\frac{d\phi}{2\pi}\frac{1}{a+b\cos\phi}=\frac{1}{\sqrt{a^2-b^2}},\qquad a>b>0,$$

$$\int_0^{2\pi}\frac{d\phi}{2\pi}\frac{\ln(a+b\cos\phi)}{a+b\cos\phi}=\frac{1}{\sqrt{a^2-b^2}}\ln\frac{2(a^2-b^2)}{a+\sqrt{a^2-b^2}},$$

we obtain

$$I_s=(1-x)x\int_1^{\rho^2}\frac{dz_2}{z_2^2}\int_{x^2}^{x^2\rho^2}dz_l\times\frac{\ln(z_2^2(1-x)x^3)-\ln[(z_1-z_2x^2)^2+4\sigma^2x^2(1-x)^2z_2]}{\sqrt{(z_1-x^2z_2)^2+4\sigma^2x^2(1-x)^2z_2}}.$$

Since we are working with logarithmic accuracy, in the integration over z_1 we can consider only the region $|z_1-x^2z_2|<\eta$, $\sigma^2\ll\eta\ll 1$. We obtain

$$I_s=x(1-x)\int_1^{\rho^2}\frac{dz_2}{z_2^2}L\left[\frac{1}{2}L+\ln\frac{x}{1-x}\right].$$

The other integrals are calculated similarly:

$$I_t=-(1-x)\int_1^{\rho^2x^2}\frac{dz_2}{z_2^2}L\left[\frac{1}{2}L+\ln\frac{1}{1-x}\right],$$

$$i_s=x(1-x)\int_1^{\rho^2}\frac{dz_2}{z_2^2}L,$$

$$i_t=-(1-x)\int_1^{\rho^2x^2}\frac{dz_2}{z_2^2}L,\quad m_s=x^2\int_1^{\rho^2}\frac{dz_2}{z_2^2},$$

$$m_t=\int_1^{\rho^2x^2}\frac{dz_2}{z_2^2}.$$

Now we can write the T contribution in its final form:

$$\Sigma_T^{H(S+V)}=\frac{1}{2}\left(\frac{\alpha}{\pi}\right)^2\int_1^{\rho^2}\frac{dz}{z^2}L\int_{x_c}^{1-\Delta}dx\,\frac{1+x^2}{1-x}\left\{\left(\frac{1}{2}L+\ln\frac{x}{1-x}\right)\ln x-\mathrm{Li}_2(1-x)+\frac{x^2+2x-1}{4(1+x^2)}-\frac{2x\ln x}{1+x^2}-\Theta(x^2\rho^2-z)\left[\left(\frac{1}{2}L+\ln\frac{1}{1-x}\right)\ln x-\frac{1}{2}\ln^2 x-\mathrm{Li}_2(1-x)-\frac{1+2x-x^2}{4(1+x^2)}-\frac{2x\ln x}{1+x^2}\right]\right\}.$$

Then the total contribution of the emission of a single hard photon from an electron line including virtual one-loop corrections and accompanied by the emission of a soft photon can be written as the sum

$$\Sigma^{H(S+V)}=\Sigma_\eta^{H(S+V)}+\Sigma_T^{H(S+V)},$$

which is given in Eq. (42).

APPENDIX C: CONTRIBUTION OF THE SEMICOLLINEAR KINEMATICS OF TWO-PHOTON EMISSION FROM A SINGLE LEPTON LINE

An alternative use of the quasireal-electron approximation[26] is the direct calculation of the contributions of various graphs. Since here we are working with logarithmic accuracy, we can restrict ouselves to the consideration of two semicollinear regions: (1) when the photon with 4-momentum k_1 is emitted in a cone of angle no larger than $\theta_0\ll 1$ about the direction of motion of the initial electron; and (2) when the photon with momentum k_1 is emitted in such a cone about the direction of motion of the scattered electron. In both cases it is assumed that the second photon does not reach any of these cones. Taking into account the identical nature of the photons by means of the statistical factor 1/2!, we obtain the differential cross section in the form

$$d\sigma_{SC}^{HH}=\frac{\alpha^4}{2\pi}\int\frac{d^2\mathbf{q}_2^\perp}{\pi(\mathbf{q}_2^\perp)^4}\int\frac{d^2\mathbf{q}_1^\perp}{\pi}\int_{x_c}^{1-2\Delta}dx\int_\Delta^{1-x-\Delta}\times\frac{dx_1dx_2}{x_1x_2x}\delta(1-x_1-x_2-x)\int R\,\frac{d^2\mathbf{k}_1^\perp}{\pi},\tag{86}$$

where

$$Q_1^{-4}\int R\,\frac{d^2\mathbf{k}_1^\perp}{\pi}$$

$$=2(\mathbf{q}_2^\perp)^2\int\frac{d^2\mathbf{k}_1^\perp}{\pi}$$

$$\times\left\{\frac{[1+(1-x_1)^2][x^2+(1-x_1)^2]}{x_1(1-x_1)^2(2p_1k_1)(2p_1k_2)(2q_1k_2)}\Bigg|_{\mathbf{k}_1\|\mathbf{p}_1}\right.$$

$$\left.+\frac{x[1+(1-x_2)^2][x^2+(1-x_2)^2]}{x_1(1-x_2)^2(2q_1k_1)(2p_1k_2)(2q_1k_2)}\Bigg|_{\mathbf{k}_1\|\mathbf{q}_1}\right\}.$$

In the case of emission of a collinear photon with momentum $\mathbf{k}_1$ along the momentum $\mathbf{p}_1$, it is convenient to write the kinematic invariants as

$$2p_1k_1=\frac{Q_1^2}{x_1}[(\mathbf{k}_1^\perp)^2+\sigma^2x_1^2],\quad 2p_1k_2=\frac{Q_1^2}{x_2}(\mathbf{k}_2^\perp)^2,$$

$$2q_1k_2=\frac{Q_1^2}{x_2x}[x\mathbf{q}_2^\perp-(1-x_1)\mathbf{q}_1^\perp]^2,\quad \mathbf{k}_2^\perp=-\mathbf{q}_2^\perp-\mathbf{q}_1^\perp,$$

and in the case of emission along $\mathbf{q}_1$ they can be written as

$$2k_1q_1=\frac{Q_1^2}{x_1x}[\sigma^2x_1^2+(x\mathbf{k}_1^\perp-\mathbf{q}_1^\perp)^2],\quad 2p_1k_2=\frac{Q_1^2}{x_2}(\mathbf{k}_2^\perp)^2,$$

$$2q_1k_2=\frac{Q_1^2}{x_2x}(\mathbf{q}_1^\perp-x\mathbf{q}_2^\perp)^2,\quad \mathbf{k}_2^\perp=\mathbf{q}_2^\perp-\mathbf{q}_1^\perp\frac{1-x_2}{x},$$

where $Q_1^2=\varepsilon^2\theta_1^2$, $\sigma^2=m^2/Q_1^2$, and we have introduced the dimensionless vectors $\mathbf{k}_2^\perp$, $\mathbf{q}_1^\perp$, and $\mathbf{q}_2^\perp$ such that $(\mathbf{q}_1^\perp)^2=z_1$, $(\mathbf{q}_2^\perp)^2=z_2$, and $\widehat{\mathbf{q}_1^\perp\mathbf{q}_2^\perp}=\phi$.

The integration over $d^2\mathbf{k}_1^\perp$ is carried out with single-logarithmic accuracy:

$$Q_1^2\int\frac{d^2\mathbf{k}_1^\perp}{\pi(2p_1k_1)}\Bigg|_{\mathbf{k}_i\|\mathbf{p}_i}=x_1L,$$

$$Q_1^2\int\frac{d^2\mathbf{k}_1^\perp}{\pi(2q_1k_1)}\Bigg|_{\mathbf{k}_i\|\mathbf{q}_i}=\frac{x_1}{x}L.$$

At this stage it is necessary to consider the kinematic constraints on the integration variables ϕ and z_1. Let us consider the conditions on the emission angle of the second photon:

$$\left|\frac{\mathbf{k}_2^\perp}{x_2}\right|>\theta_0,\quad \left|\frac{\mathbf{q}_1^\perp}{x}-\frac{\mathbf{k}_2^\perp}{x_2}\right|>\theta_0.$$

The first condition does not allow the photon to enter into the collinear cone about the direction of motion of the initial electron, and the second does the same for the final electron. They can be written as a set of conditions in terms of the variables z_1 and ϕ:

i) $1>\cos\phi>-1+\dfrac{\lambda^2-(\sqrt{z_1}-\sqrt{z_2})^2}{2\sqrt{z_1z_2}}$,

$|\sqrt{z_1}-\sqrt{z_2}|<\lambda$,

ii) $1>\cos\phi>-1$, $|\sqrt{z_1}-\sqrt{z_2}|>\lambda$,

iii) $1>\cos\phi>-1+\left[\dfrac{x^2}{(1-x_1)^2}\lambda^2-\left(\sqrt{z_1}-\dfrac{x}{1-x_1}\sqrt{z_2}\right)^2\right]\Big/2\sqrt{z_1z_2}\,\dfrac{x}{1-x_1}$,

$\left|\sqrt{z_1}-\dfrac{x\sqrt{z_2}}{1-x_1}\right|<\lambda\,\dfrac{x}{1-x_1}$,

iv) $1>\cos\phi>-1$, $\left|z_1-\dfrac{x^2}{(1-x_1)^2}z_2\right|>2\lambda\sqrt{z_2}\,\dfrac{x^2}{(1-x_1)^2}$,

where $\lambda=x_2\theta_0/\theta_1$. We assume that $\lambda\ll1$. Actually, for the parameter θ_0 determining the region of the collinear kinematics we have $\theta_0\varepsilon\gg m$ or $\theta_0\gg10^{-5}$ for the energy of the LEP I collider. On the other hand, we have the experimental bounds on the parameter θ_1: $\theta_1\gtrsim10^{-2}$. This allows us to assume that $\lambda\ll1$ within our accuracy.

In a similar way we can obtain the limits on the region of integration also for the case where the photon of momentum k_1 enters the collinear cone about the direction of motion of the scattered electron.

In regions (ii) and (iv) we can perform the integration over the azimuthal angle:

$$\int_0^{2\pi}\frac{d\phi}{2\pi(2p_1k_2)(2q_1k_2)}\Bigg|_{\mathbf{k}_1\|\mathbf{p}_1}=\frac{x_2xQ_1^{-4}}{(1-x_1)z_1-xz_2}\left[\frac{1}{|z_2-z_1|}-\frac{x(1-x_1)}{|x^2z_2-(1-x_1)^2z_1|}\right],$$

$$\int_0^{2\pi}\frac{d\phi}{2\pi(2p_1k_2)(2q_1k_2)}\Bigg|_{\mathbf{k}_1\|\mathbf{q}_1}=\frac{x_2x^3(1-x_2)^{-2}Q_1^{-4}}{z_1-z_2\dfrac{x^2}{1-x_2}}\left[\frac{1}{\left|z_1-z_2\dfrac{x^2}{(1-x_2)^2}\right|}-\frac{1-x_2}{|z_1-x^2z_2|}\right].$$

In regions (i) and (iii) we have

$$\mathcal{I}=\int dz_1\int\frac{d\phi}{2\pi(z_1+z_2+2\sqrt{z_1z_2}\cos\phi)}\Bigg|_{|\sqrt{z_1}-\sqrt{z_2}|<\lambda}=\frac{2}{\pi}\int\frac{dz}{|z_1-z_2|}\arctan\left\{\frac{(\sqrt{z_1}-\sqrt{z_2})^2}{|z_1-z_2|}\tan\frac{\phi_0}{2}\right\},$$

where

$$\phi_0=\arccos\left(-1+\frac{\lambda^2-(\sqrt{z_1}-\sqrt{z_2})^2}{2\sqrt{z_1z_2}}\right).$$

As a result, we obtain

$$\mathscr{T}=2\ln 2.$$

Then the complete expression for the contribution of the semicollinear kinematic region is written as

$$d\sigma_{SC}^{HH}=\frac{\alpha^2}{4\pi^2}\int_{x_c}^{1-2\Delta}dx\int_{\Delta}^{1-x-\Delta}\times\frac{dx_1dx_2\delta(1-x-x_1-x_2)}{x_1x_2(1-x_1)^2}[1+(1-x_1)^2][x^2+(1-x_1)^2]\int_1^{\rho^2}\frac{dz}{z^2}L\Bigg\{\ln\frac{z\theta_1^2}{\theta_0^2}[1+\Theta(\rho^2x^2-z)+2\Theta(\rho^2(1-x_1)^2-z)]+\Theta(\rho^2x^2-z)\ln\frac{(z-x^2)(\rho^2x^2-z)}{x^2(z-x(1-x_1))(\rho^2x(1-x_1)-z)}+\Theta(z-\rho^2(1-x_1)^2)\times\Bigg[\ln\frac{(z-\rho^2(1-x_1)x)(z-(1-x_1)^2)}{(\rho^2(1-x_1)^2-z)(z-x(1-x_1))}+\ln\frac{(\rho^2(1-x_1)-z)(z-(1-x_1)^2)}{(\rho^2(1-x_1)^2-z)(z-(1-x_1))}\Bigg]+\Theta(z-\rho^2x^2)\ln\frac{(z-\rho^2x(1-x_1))(z-x^2)}{(\rho^2x^2-z)(z-x(1-x_1))}+\Theta(\rho^2(1-x_1)^2-z)\times\Bigg[\ln\frac{(z-(1-x_1)^2)(\rho^2(1-x_1)^2-z)}{(\rho^2x(1-x_1)-z)(z-x(1-x_1))(1-x_1)^2}+\ln\frac{(z-(1-x_1)^2)(\rho^2(1-x_1)^2-z)}{(\rho^2(1-x_1)-z)(z-(1-x_1))(1-x_1)^2}\Bigg]+\ln\frac{(z-1)(\rho^2-z)}{(z-(1-x_1))(\rho^2(1-x_1)-z)}\Bigg\}.$$

In order to confirm the cancellation of the auxiliary parameter θ_0/θ_1, we consider the corresponding part of the contribution of the collinear kinematics:

$$\Sigma_{\rm coll}^{HH}=\frac{\alpha^2}{4\pi^2}\int_{x_c}^{1-2\Delta}dx\int_{\Delta}^{1-x-\Delta}\times\frac{dx_1dx_2\delta(1-x-x_1-x_2)}{x_1x_2(1-x_1)^2}[1+(1-x_1)^2][x^2+(1-x_1)^2]\int_1^{\rho^2}\frac{dz}{z^2}\left(L^2-2L\ln\frac{z\theta_1^2}{\theta_0^2}\right)\left[\frac{1}{2}+\frac{1}{2}\Theta(\rho^2x^2-z)+\Theta(\rho^2(1-x_1)^2-z)\right]+\cdots.$$

The full sum of the contributions of the two kinematics for the emission of two hard photons from an electron line is given in Eq. (46).

APPENDIX D: CANCELLATION OF THE Δ DEPENDENCE IN THE NONLEADING CONTRIBUTIONS

Let us consider the nonleading contributions to $\Sigma^{2\gamma}$ which are singular for $\Delta\to 0$. Dropping the common factor $(\alpha/\pi)^2\mathscr{L}\int dz/z^2$, we give the individual contributions below.

Let us first consider the contributions to $\Sigma^{\gamma\gamma}$. The corrections associated with virtual and soft photons give

$$(\Sigma^{VV+VS+SS})_\Delta=\ln\Delta(-7-4\ln\Delta)(1,\rho^2), \tag{87}$$

where we use (a,b) to denote the limits of the integration over z: $(a,b)=\Theta(z-a)\Theta(b-z)$. The contribution of virtual and soft corrections to the emission of a single hard photon gives

$$(\Sigma^{H(S+V)})_\Delta=\frac{1}{2}\ln\Delta\Bigg\{(1,\rho^2)(16\ln\Delta+14)+4\int_{\tilde{x}_c}^1dx\,\frac{1+x^2}{1-x}[(1,\rho^2)-(1,\rho^2x^2)]+4\Bigg[-2\ln(1-x_c)-2\ln(1-\tilde{x}_c)+\int_{x_c}^1dx(1+x)+\int_{\tilde{x}_c}^1dx(1+x)\Bigg]+2\int_{x_c}^1dx\,\frac{1+x^2}{1-x}[(1,\rho^2)-(1,\rho^2x^2)]\ln x+2\int_{x_c}^1dxk(x,z)\,\frac{1+x^2}{1-x}\Bigg\}, \tag{88}$$

where $\tilde{x}_c=\max(x_c,1/\rho)$, and $k(x,z)$ is given in (21). The singular contribution associated with the emission of two hard photons has the form [see (46)]

$$(\Sigma^{HH})_\Delta=\ln\Delta\Bigg\{\int_{x_c}^1dx\,\frac{1+x^2}{1-x}[-(1,\rho^2)L_1-(1,\rho^2x^2)L_2-((1,\rho^2)-(1,\rho^2x^2))L_3]-\int_{x_c}^1dx(3+x)-\int_{\tilde{x}_c}^1dx(3+x)-4\ln\Delta+4\ln(1-x_c)+4\ln(1-\tilde{x}_c)-\int_{\tilde{x}_c}^1dx\,\frac{1+x^2}{1-x}[(1,\rho^2)-(1,\rho^2x^2)]\Bigg\}. \tag{89}$$

Now it is easy to verify that these contributions cancel each other:

$$(\Sigma^{VV+VS+SS})_\Delta+(\Sigma^{H(S+V)})_\Delta+(\Sigma^{HH})_\Delta=0. \tag{90}$$

Let us now consider the corresponding contributions to Σ_γ^γ:

$$(\Sigma_{S+V}^{S+V})_\Delta=\ln\Delta(-14-8\ln\Delta)(1,\rho^2),$$

$$(\Sigma^H_{S+V}+\Sigma^{S+V}_H)_\Delta=\ln\Delta\Bigg\{2\int_{x_c}^1 dx\,\frac{1+x^2}{1-x}\,k(x,z)+(1,\rho^2)\times\Bigg[16\ln\Delta+14-8\ln(1-x_c)-8\ln(1-\tilde{x}_c)+4\int_{x_c}^1 dx(1+x)+4\int_{\tilde{x}_c}^1 dx(1+x)\Bigg]+4\int_{\tilde{x}_c}^1 dx\,\frac{1+x^2}{1-x}[(1,\rho^2)-(1,\rho^2x^2)]\Bigg\},$$

$$(\Sigma^H_H)_\Delta=\ln\Delta\Bigg\{-8(1,\rho^2)[\ln\Delta-\ln(1-x_c)-\ln(1-\tilde{x}_c)]-8\int_{\tilde{x}_c}^1 dx\,\frac{[(1,\rho^2)-(1,\rho^2x^2)]}{1-x}-2\int_{x_c}^1 dx\,k(x,z)\,\frac{1+x^2}{1-x}-4\int_{x_c}^1 dx(1+x)\times[(1,\rho^2)+(1,\rho^2x^2)]\Bigg\}. \tag{91}$$

Transforming the last term in $(\Sigma^H_H)_\Delta$ using the identity

$$-4\int_{x_c}^1 dx(1+x)[(1,\rho^2)+(1,\rho^2x^2)]=-4\int_{x_c}^1 dx(1+x)\times(1,\rho^2)-4\int_{\tilde{x}_c}^1 dx(1+x)(1,\rho^2)+4\int_{\tilde{x}_c}^1 dx(1+x)\times[(1,\rho^2)-(1,\rho^2x^2)], \tag{92}$$

we again confirm the cancellation of the Δ dependence:

$$(\Sigma^{S+V}_{S+V})_\Delta+(\Sigma^H_{S+V}+\Sigma^{S+V}_H)_\Delta+(\Sigma^H_H)_\Delta=0. \tag{93}$$

APPENDIX E: REPRESENTATION OF THE LEADING CONTRIBUTIONS TO $\Sigma^{\gamma\gamma}$ IN TERMS OF KERNELS OF THE EVOLUTION EQUATIONS

Here we shall show that the leading-log contributions can be represented in the form predicted by the renormalization group. The sum of the above contributions to $\Sigma^{\gamma\gamma}$ minus the leading terms can be written as

$$\Sigma^{\gamma\gamma}=2\left(\frac{\alpha}{\pi}\right)^2\mathscr{L}^2\int_1^{\rho^2}\frac{dz}{z^2}\Bigg\{2\int_{x_c}^1 dx\,\delta(1-x)\left(\ln^2\Delta+\frac{3}{2}\ln\Delta+\frac{9}{16}\right)+\frac{1}{2}\int_{x_c}^{1-\Delta}dx\,\frac{1+x^2}{1-x}\left(2\ln\Delta-\ln x+\frac{3}{2}\right)(1+\Theta(x^2\rho^2-z))+\frac{1}{4}\int_{x_c}^{1-2\Delta}dx\left[2\frac{1+x^2}{1-x}\ln\frac{1-x-\Delta}{\Delta}+\frac{1}{2}(1+x)\ln x-1+x\right][1+3\Theta(x^2\rho^2-z)]+\frac{1}{4}\int_{x_c}^1 dx\left[2\frac{1+x^2}{1-x}\ln\left(\frac{1-x-\Delta}{\Delta}\,\frac{\rho-\sqrt{z}}{\sqrt{z}-\rho x}\,\sqrt{x}\right)+x-1-\frac{1}{2}(1+x)\ln\frac{\rho^2}{z}+\frac{\sqrt{z}}{\rho}-\frac{x\rho}{\sqrt{z}}\right]\Theta(-x^2\rho^2+z)\Bigg\}. \tag{94}$$

It can be checked that the Δ dependence cancels in this expression. We shall show below that this expression can be written as

$$\Sigma^{\gamma\gamma}=\frac{1}{2}\left(\frac{\alpha\mathscr{L}}{\pi}\right)^2\int_1^{\rho^2}\frac{dz}{z^2}\int_{x_c}^1 dx\Bigg\{\frac{1}{2}P^{(2)}(x)[1+\Theta(x^2\rho^2-z)]+\int_x^1 dt\,\frac{1}{t}P(t)P\left(\frac{x}{t}\right)\Theta(t^2\rho^2-z)\Bigg\}, \tag{95}$$

where the kernels of the evolution equations (see Appendix G) P and $P^{(2)}$ are given above [see (24) and (50)]. For this we transform Eq. (95), using the substitution

$$\Theta(t^2\rho^2-z)=\frac{1}{2}(1+\Theta(x^2\rho^2-z))+\frac{1}{2}\Theta(z-x^2\rho^2)-\Theta(z-t^2\rho^2),$$

and change the order of integration in the last term:

$$\int_x^1 dt\int_{\rho^2t^2}^{\rho^2}dz=\int_{x^2\rho^2}^{\rho^2}dz\int_x^{\sqrt{z}/\rho}dt=\int_1^{\rho^2}dz\,\Theta(z-\rho^2x^2)\int_x^{\sqrt{z}/\rho}dt.$$

Performing the elementary integration over t and using the explicit expressions for the kernels, it is easily verified that (95) and (94) are identical. The validity of the representation (51) for Σ^γ_γ can be verified in a similar manner.

APPENDIX F: THE CASE OF NONSYMMETRIC DETECTORS

For definiteness, we shall assume that the scattered electron is detected by a ring counter with aperture

$$\theta_1<\theta_{e^-}<\theta_3,$$

and the positron by one with narrower aperture:

$$\theta_2<\theta_{e^+}=\theta_4,$$

where

$$1<\rho_2<\rho_4<\rho_3,\quad \rho_{2,3,4}=\theta_{2,3,4}/\theta_1.$$

This ordering is typical of experiments at LEP I. Calculations similar to those of Appendix A give the following for the contribution of the emission of a single hard photon:

$$\Sigma^{H(W)}+\Sigma_{H(N)}=\frac{1}{2}\left(\frac{\alpha}{\pi}\right)\int_{x_e}^{1-\Delta}dx\,\frac{1+x^2}{1-x}\int_1^{\rho_3^2}\frac{dz}{z^2}(1-\Pi(-zQ_1^2))^{-2}\{A+B+C+D\},$$

$$A=[\Theta(\rho_2-x\rho_3)(\rho_2^2,\rho_4^2)+\Theta(x\rho_3-\rho_2)\Theta(\rho_4-x\rho_3)\times(x^2\rho_3^2,\rho_4^2)]\ln\left|\frac{(x\rho_3^2-z)(z-x^2)}{(x^2\rho_3^2-z)(z-x)}\right|+(\rho_2^2,\rho_4^2)\times(x^2,x^2\rho_3^2)\left[L-1+\frac{(1-x)^2}{1+x^2}+\ln\left|\frac{(x^2\rho_3^2-z)(z-x^2)}{x^2(x\rho_3^2-z)(z-x)}\right|\right],$$

$$B=(\rho_2^2,\rho_4^2)\left[L-1+\frac{(1-x)^2}{1+x^2}+\ln\left|\frac{x^2(\rho_3^2-z)(z-1)}{(x\rho_3^2-z)(z-x)}\right|\right],$$

$$C=[-((1,x^2\rho_2^2)-(x^2\rho_4^2,\rho_3^2))\Theta(x\rho_2-1)+(1,\rho_3^2)\Theta(1-x\rho_4)+(x^2\rho_4^2,\rho_3^2)\Theta(1-x\rho_2)\Theta(x\rho_4-1)]\ln\left|\frac{(x\rho_4^2-z)(z-x^2\rho_2^2)}{(x^2\rho_4^2-z)(z-x\rho_2^2)}\right|+(1,\rho_3^2)(x^2\rho_2^2,x^2\rho_4^2)\left[L-1+\frac{(1-x)^2}{1+x^2}+\ln\left|\frac{(x^2\rho_4^2-z)(z-x^2\rho_2^2)}{x^2(x\rho_4^2-z)(z-x\rho_2^2)}\right|\right],$$

$$D=-[(1,\rho_2^2)-(\rho_4^2,\rho_3^2)]\ln\left|\frac{(x\rho_4^2-z)(z-\rho_2^2)}{(\rho_4^2-z)(z-x\rho_2^2)}\right|+(\rho_2^2,\rho_4^2)\times\left[L-1+\frac{(1-x)^2}{1+x^2}+\ln\left|\frac{x^2(\rho_4^2-z)(z-\rho_2^2)}{(x\rho_4^2-z)(z-x\rho_2^2)}\right|\right]. \quad (96)$$

The terms A, B, C, and D respectively correspond to the contributions from emission by the initial electron, the final electron, and the initial and final positrons. We note that for $\rho_2=1$ and $\rho_4=\rho_3=\rho$ the result given above becomes Eq. (21).

Taking into account the corrections associated with the emission of virtual and soft photons, the correction can be written as follows in first-order perturbation theory:

$$(\Sigma^{\gamma})^{NW}=\frac{\alpha}{2\pi}\int_1^{\rho_2^3}\frac{dz}{z^2}(1-\Pi(-zQ_1^2))^{-2}\left\{-2+\int_{x_c}^1 dx\;P(x)[(\rho_2^2,\rho_4^2)((1,\rho_3^2)+(x^2,x^2\rho_3^2))+(1,\rho_3^2)((\rho_2^2,\rho_4^2)+(x^2\rho_2^2,x^2\rho_4^2))]+\int_{x_c}^1 dx\;k(x,z)^{NW}\frac{1+x^2}{1-x}\right\},$$

where $k(x,z)^{NW}$ is obtained from the expression in curly brackets in (96) by discarding the terms proportional to $(L-1)$.

We also give the expressions for the contributions of second-order perturbation theory in the leading-log approximation:

$$(\Sigma_{\gamma}^{\gamma})^{NW}=\frac{1}{4}\left(\frac{\alpha}{\pi}\right)^2\int_{x_c^2}^{\rho_4^2}\frac{dz}{z^2}L^2(1-\Pi(-zQ_1^2))^{-2}\int_{x_c}^1 dx_1\int_{x_c/x_1}^1 dx_2P(x_1)P(x_2)\times[(1,\rho_3^2)+(x_1^2,x_1^2\rho_3^2)][(\rho_2^2,\rho_4^2)+(x_2^2\rho_2^2,x_2^2\rho_4^2)],$$

$$(\Sigma^{\gamma\gamma})^{NW}=\frac{1}{4}\left(\frac{\alpha}{\pi}\right)^2\int_1^{\rho_4^2}\frac{dz}{z^2}L^2(1-\Pi(-zQ_1^2))^{-2}\int_{x_c}^1 dx\left\{\frac{1}{2}P^{(2)}(x)[(\rho_2^2,\rho_4^2)\times((1,\rho_3^2)+(x^2,x^2\rho_3^2))+(1,\rho_3^2)((\rho_2^2,\rho_4^2)+(x^2\rho_2^2,x^2\rho_4^2))]+\int_x^1\frac{dt}{t}P(t)P\left(\frac{x}{t}\right)\times[(\rho_2^2,\rho_4^2)(1,t^2\rho_3^2)+(1,\rho_3^2)(\rho_2^2,t^2\rho_4^2)]\right\},$$

$$(\Sigma^{e^+e^-})^{NW}=\frac{1}{8}\left(\frac{\alpha}{\pi}\right)^2\int_1^{\rho_4^2}\frac{dz}{z^2}L^2(1-\Pi(-zQ_1^2))^{-2}\int_{x_c}^1 dx\,R(x)[(\rho_2^2,\rho_4^2)\times((1,\,\rho_3^2)+(x^2,x^2\rho_3^2))+(1,\rho_3^2)((\rho_2^2,\rho_4^2)+(x^2\rho_2^2,x^2\rho_4^2))].$$

APPENDIX G: ITERATION OF THE LIPATOV EQUATIONS

The cross section for the process

$$e^+(p_+)+e^-(p_-)\to\gamma^*\to\text{hadrons}$$

taking into account the radiative corrections to the initial state can be written as the cross section for the Drell–Yan process:

$$\sigma^{e\bar{e}\to h}(s)=\int^1 dx_1\int^1 dx_2\Theta\left(-2+\frac{\Delta\varepsilon}{\varepsilon}+x_1+x_2\right)\mathscr{D}_e^e(x_1)\mathscr{D}_{\bar{e}}^{\bar{e}}(x_2)\sigma_0^{e\bar{e}\to h}(x_1x_2s)(1-\Pi(x_1x_2s))^{-2}K,$$

where σ_0 is the cross section neglecting radiative corrections,

$$\Pi(s)=\frac{\alpha}{3\pi}\left(\ln\frac{s}{m^2}-\frac{5}{9}\right),$$

and K is a factor taking into account the nonleading corrections,

$$K=1+\frac{\alpha}{\pi}\left(\frac{\pi^2}{3}-\frac{1}{2}\right).$$

The structure functions $\mathscr{D}_a^b(x)$ describe the probability of finding a particle of type b with momentum fraction x in a particle of type a. They satisfy the Lipatov equations:[11]

$$\mathscr{D}_e^e(x,s)=\delta(1-x)+\int_{m^2}^{s}\frac{dt\alpha(t)}{2\pi t}\left[\int_x^1\frac{dy}{y}\mathscr{D}_e^e(y,t)P_e^e\left(\frac{x}{y}\right)+\int_x^1\frac{dy}{y}\mathscr{D}_e^\gamma(y,t)P_\gamma^e\left(\frac{x}{y}\right)\right],$$

$$\mathscr{D}_e^{\bar{e}}(x,s)=\int_{m^2}^{s}\frac{dt\alpha(t)}{2\pi t}\left[\int_x^1\frac{dy}{y}\mathscr{D}_e^{\bar{e}}(y,t)P_{\bar{e}}^{\bar{e}}\left(\frac{x}{y}\right)+\int_x^1\frac{dy}{y}\mathscr{D}_e^\gamma(y,t)P_\gamma^{\bar{e}}\left(\frac{x}{y}\right)\right],$$

$$\mathscr{D}_e^\gamma(x,s)=-\frac{2}{3}\int_{m^2}^{s}\frac{dt\alpha(t)}{2\pi t}\mathscr{D}_e^\gamma(x,t)+\int_{m^2}^{s}\frac{dt\alpha(t)}{2\pi t}\left[\int_x^1\frac{dy}{y}\mathscr{D}_e^e(y,t)P_{\bar{e}}^\gamma\left(\frac{x}{y}\right)+\int_x^1\frac{dy}{y}\mathscr{D}_e^{\bar{e}}(y,t)P_{\bar{e}}^\gamma\left(\frac{x}{y}\right)\right],$$

where

$$\alpha(t)=\alpha\left(1-\frac{\alpha}{3\pi}\ln\frac{t}{m^2}\right)^{-1},$$

$$P_\gamma^e(z)=P_\gamma^{\bar{e}}(z)=z^2+(1-z)^2,$$

$$P_e^e(z)=P_{\bar{e}}^{\bar{e}}(z)\equiv P(z)=\lim_{\Delta\to 0}\left\{\Theta(1-z-\Delta)\frac{1+z^2}{1-z}+\delta(1-z)\left(\frac{3}{2}+2\ln\Delta\right)\right\},$$

$$P_e^\gamma(z)=P_{\bar{e}}^\gamma(z)=\frac{1}{z}(1+(1-z)^2).$$

It is convenient to write $\mathscr{D}_e^e$ as the sum of singlet and nonsinglet contributions:

$$\mathscr{D}_e^e=\mathscr{D}_{NS}+\mathscr{D}_S.$$

One of these, $\mathscr{D}_{NS}$, can be expanded in a functional series:

$$\mathscr{D}_{NS}(x,\beta)=\delta(1-x)+\sum_{k=1}^{\infty}\frac{1}{k!}\left(\frac{\beta}{4}\right)^k P^{*k}(x),$$

$$\beta=\frac{2\alpha}{\pi}L,$$

$$P^{*k}(x)=\underbrace{P(\bullet)\otimes P(\bullet)\otimes\ldots\otimes P(x)}_{k},$$

$$P_1(\bullet)\otimes P_2(x)=\int_0^1 dx_1dx_2\delta(x-x_1x_2)P_1(x_1)P_2(x_2)=\int_x^1\frac{dy}{y}P_1(y)P_2\left(\frac{x}{y}\right).$$

The explicit expressions for the kernels $P^{(2)}(x)$ and $P^{(3)}(x)$ are given above in the text of the review. We note an important property of the $P^{(k)}(x)$:

$$\int_0^1 dxP^{(k)}(x)=0,\quad k=1,2,\ldots. \tag{97}$$

For the iterations it is convenient to introduce new functions, following Ref. 24:

$$\mathscr{D}_S=\mathscr{D}_e^{\bar{e}},\quad \mathscr{D}_{NS}=\mathscr{D}_e^e-\mathscr{D}_S,\quad \mathscr{D}_+=\mathscr{D}_e^e+\mathscr{D}_e^{\bar{e}}.$$

These functions satisfy the following system of equations:

$$\frac{\partial}{\partial\beta}\mathscr{D}_e^\gamma=-\frac{\beta}{6}\mathscr{D}_e^\gamma+\frac{\beta}{4}\mathscr{D}_+\otimes P_e^\gamma,$$

$$\mathscr{D}_+(x,\beta)=\delta(1-x)+\frac{1}{4}\int_0^\beta d\eta\left\{\mathscr{D}_+(\bullet,\eta)\otimes P(x)+\frac{1}{2}\exp\left(-\frac{\eta}{6}\right)\int_0^\eta dy\exp\left(\frac{y}{6}\right)\mathscr{D}_+(\bullet,y)\otimes R(x)\right\},$$

$$R(x)=P_e^\gamma(\bullet)\otimes P_\gamma^e(x)=\frac{1-x}{3x}(4+7x+4x^2)+2(1+x)\ln x\equiv R_s(x).$$

For $\mathscr{D}_S(x,\beta)$ we have

$$\mathscr{D}_S=\frac{\beta^2}{32}R(x)+\frac{\beta^3}{6}\left[\frac{1}{32}P(\bullet)\otimes R(x)-\frac{1}{96}R(x)\right].$$

We conclude by noting that the function $f(z)$ relating the cross sections for processes producing a system of final particles X with invariant mass W in collisions of e^+e^- beams and photon beams is the convolution of two evolution kernels:

$$\sigma^{e\bar{e}\to e\bar{e}X}(s)\approx\left(\frac{\alpha}{2\pi}L\right)^2\int_{z_{\rm th}}^1\frac{dz}{z}f(z)\sigma^{\gamma\gamma\delta X}(zs),$$

$$f(z)=\int_z^1\frac{dx}{x}(1+(1-x)^2)\left(1+\left(1-\frac{z}{x}\right)^2\right)=(2+z)^2\ln\frac{1}{z}-2(1-z)(3+z),$$

$$f(z)=P_c^\gamma(\bullet)\otimes P_{\bar{c}}^\gamma(z),\quad L=\ln\frac{s}{m_e^2},\quad z_{\rm th}=\frac{W^2}{s}.$$

[1)]In a recent study,[18] a violation of the generalized eikonal representation was found at the two-loop level. We do not agree with this finding, because the authors of that study dealt with the academic problem of a massive photon.

[1] *Reports of the Working Groups on Precision Calculations for the Z Resonance*, edited by D. Bardin, W. Holik, and G. Passarino, CERN Yellow Report, CERN 95-03 (1995).

[2] S. Jadach, M. Melles, W. Placzek *et al.*, CERN Yellow Report, CERN 95-03 (1995), p. 343 and references therein.

[3] S. Jadach, E. Richter-Wąs, B. F. L. Ward, and Z. Wąs, Comput. Phys. Commun. **70**, 305 (1992); **79**, 503 (1994).

[4] A. Arbuzov, V. Fadin, E. Kuraev *et al.*, CERN Yellow Report, CERN 95-03 (1995), p. 369; V. Fadin, E. Kuraev, L. Lipatov *et al.*, in *Proc. of the Tennessee Intern. Symp. on Radiative Corrections.*, edited by B. F. L. Ward, 1994, p. 168.

[5] M. Cacciari, G. Montagna, O. Nicrosini, and F. Piccini, CERN Yellow Report, CERN 95-03 (1995), p. 389 and references therein.

[6] M. Caffo, H. Czyž, and E. Remiddi, Phys. Lett. B **327**, 369 (1994); Int. J. Mod. Phys. **4**, 591 (1993); Nuovo Cimento A **105**, 277 (1992).

[7] D. R. Yennie, S. Frautschi, and H. Suura, Ann. Phys. (N.Y.) **13**, 379 (1961).

[8] F. A. Berends, R. Kleiss, P. De Gausmaecker *et al.*, Phys. Lett. B **103**, 124 (1981); F. A. Berends *et al.*, Nucl. Phys. **B206**, 61 (1982); **B253**, 537 (1983); **B264**, 243 (1984).

[9] V. N. Baier, V. S. Fadin, V. A. Khoze, and E. A. Kuraev, Phys. Rep. **78**, 294 (1981); V. M. Budnev, I. F. Ginzburg, G. V. Meledin, and V. G. Serbo, Phys. Rep. C **15**, 183 (1975).

[10] E. A. Kuraev, L. N. Lipatov, and N. P. Merenkov, Phys. Lett. **B47**, 33 (1973); Preprint No. 46, Leningrad Nuclear Physics Institute, Gatchina (1973) [in Russian]; H. Cheng and T. T. Wu, Phys. Rev. **184**, 1868 (1969); É. A. Kuraev, L. N. Lipatov, N. P. Merenkov *et al.*, Yad. Fiz. **56**, No. 11, 145 (1993) [Phys. At. Nucl. **56**, 1537 (1993)].

[11] L. N. Lipatov, Yad. Fiz. **20**, 181 (1974) [Sov. J. Nucl. Phys. **20**, 94 (1975)].

[12] G. Altarelli and G. Parisi, Nucl. Phys. **B126**, 298 (1977).

[13] É. A. Kuraev and V. S. Fadin, Yad. Fiz. **41**, 733 (1985) [Sov. J. Nucl. Phys. **41**, 466 (1985)]; Preprint 84-44, Nuclear Physics Institute, Novosibirsk (1984) [in Russian].

[14] O. Nicrosini and L. Trentadue, Phys. Lett. **B196**, 551 (1987).

[15] R. Budny, Phys. Lett. **B55**, 227 (1975); D. Bardin, W. Hollik, and T. Riemann, Preprint MPI-PAE/Pth 32/90, PHE90-9, Max Planck Institute (1990); M. Boehm, A. Denner, and W. Hollik, Nucl. Phys. **B304**, 687 (1988).

[16] R. V. Polovin, Zh. Éksp. Teor. Fiz. **31**, 449 (1956) [Sov. Phys. JETP **4**, 385 (1957)]; F. A. Redhead, Proc. R. Soc. London **220**, 219 (1953); F. A. Berends *et al.*, Nucl. Phys. **B68**, 541 (1974).

[17] F. Jegerlehner, Prog. Part. Nucl. Phys. **27**, 1 (1991).

[18] G. Fäldt and P. Osland, Report 1993-04, University of Bergen (1993).

[19] R. Barbieri, J. A. Mignaco, and E. Remiddi, Nuovo Cimento A **11**, 824 (1972).

[20] É. A. Kuraev, N. P. Merenkov, and V. S. Fadin, Yad. Fiz. **45**, 782 (1987) [Sov. J. Nucl. Phys. **45**, 486 (1987)].

[21] N. P. Merenkov, Yad. Fiz. **48**, 1782 (1988) [Sov. J. Nucl. Phys. **48**, 1073 (1988)].

[22] N. P. Merenkov, Yad. Fiz. **50**, 750 (1989) [Sov. J. Nucl. Phys. **50**, 469 (1989)].

[23] A. V. Arbuzov, E. A. Kuraev, N. P. Merenkov *et al.*, Zh. Éksp. Teor. Fiz. **108**, 3 (1995) [Sov. Phys. JETP **81**, 1 (1995)]; Preprint E2-95-110, JINR, Dubna (1995).

[24] M. Skrzypek, Acta Phys. Pol. B **23**, 135 (1992).

[25] W. Beenakker and B. Pieterzyk, Phys. Lett. **B296**, 241 (1992); **B304**, 366 (1993).

[26] J. C. Collins, D. E. Soper, and G. Sterman, in *Perturbative QCD*, edited by A. H. Müller (World Scientific, Singapore, 1989); V. N. Baier, V. S. Fadin, and V. A. Khoze, Nucl. Phys. **B65**, 381 (1973).

[27] É. A. Kuraev, N. P. Merenkov, and V. S. Fadin, Yad. Fiz. **47**, 1593 (1988) [Sov. J. Nucl. Phys. **47**, 1009 (1988)].

Translated by Patricia A. Millard